Auditory Neuroscience, Vol. 3, pp. 313–334
Reprints available directly from the publisher
Photocopying permitted by license only

Number and Axon Calibres of Cochlear Afferents in the Barn Owl

CHRISTINE KÖPPL*

Institut für Zoologie, Technische Universität München, Lichtenbergstr. 4, 85747 Garching, Germany

(Received 01 May 1996; Accepted 28 May 1996)

Afferent fibres in the auditory nerve of the barn owl were counted and their diameters measured, using a semi-automated image analysis of light-microscopical sections. Since fibres of both the basilar papilla and the lagenar macula run in the auditory nerve, but cannot be sharply distinguished, an independent evaluation of the lagenar fibres was obtained from sections near the apical end of the cochlear duct. Average numbers of 31,142 afferents from the basilar papilla and 1,342 lagenar fibres were found. Papillar axons were, on average, considerably larger than lagenar axons. Analysis of serial sections at regular intervals along the cochlea showed that less than 20% of all papillar afferents derive from regions of the basilar papilla corresponding to frequencies below 2 kHz. Above 2 kHz, about equal numbers of afferents were counted per octave. While this reflects an unusually heavy emphasis on high frequencies among birds, the afferent fibre supply is less focused on a narrow frequency band than the cochlear space map implies. Axon diameters increased systematically with frequency up to approximately 7 kHz and then decreased again towards the base of the papilla. This pattern would be suited to exaggerate latency differences between frequencies in the cochlear nucleus. However, larger axons could also be an adaptation to the increasing demands for temporal accuracy in phase locking at high frequencies. Myelination of papillar afferents was studied in ultrathin sections and found to be very uniform, with an average sheath thickness of 0.58 μm, regardless of axon diameter.

Keywords: Hearing, bird, auditory nerve, basilar papilla, time coding, innervation

Birds have become an increasingly popular model for the study of basic principles of auditory processing, both at the cochlear and more central levels. Recordings from primary afferent neurones are routinely used to study cochlear electrophysiology (e.g., Sachs *et al.*, 1974, 1980; Manley *et al.*, 1985, 1991b; Gummer, 1991; Salvi *et al.*, 1992; Smolders *et al.*, 1995). Very little, however, is known about the morphology of afferent neurones. In mammals, two classes of auditory afferents have long been known, the type I and type II afferents, innervating inner hair cells and outer hair cells, respectively. These two types differ in many respects, e.g., type I axons are myelinated whereas type II axons are not, cell bodies

*Corresponding author. Tel.: Germany 89 2891 3671. Fax: Germany 89 2891 3674. Email: ck@cipl.zoo.chemie.tu-muenchen.de.

and axons of type I neurones are larger and the two types have different targets and sizes of their terminals in the cochlear nucleus (review in Ryugo, 1992). Within the type I population, baso-apical gradients in cell body and axon size and, sometimes, myelination have been reported, as well as differences in the sizes of the peripheral and central process (Arnesen and Osen, 1978; Friede, 1984; Anniko and Arnesen, 1988; Ryugo, 1992). In the cat, morphological differences in the terminals on inner hair cells are now known to correlate with physiological subclasses of type I afferents (Ryugo, 1992). Many aspects of afferent morphology thus have potential functional importance. In addition, parameters such as fibre size will influence the success rate of electrophysiological recording, an important consideration in the interpretation of recorded data.

Studies of afferent morphology in birds have so far concentrated mainly on the synaptic terminals (reviews in Manley, 1990; Fischer, 1994a). The distribution of afferent terminals among the hair cells is known to be uneven, with an increasing number of hair cells towards the cochlear base typically being without any afferent supply at all. There is no evidence for different types of afferent synapses. Fermin and Cohen (1984) distinguished two populations of cochlear ganglion cells in the chicken, reminiscent of the mammalian types I and II, in contrast to Fischer *et al.* (1994) who found only a homogenous population. The morphology of the central afferent terminals has also been studied in detail, especially in the cochlear nucleus magnocellularis, which predominantly receives the well-known endbulbs of Held (e.g., Parks, 1981; Whitehead and Morest, 1981; Carr and Boudreau, 1991; Köppl, 1994).

The axonal morphology of avian afferents, however, is largely unknown. The average fibre or axon diameters reported for the pigeon and chicken are unusually small, being around 1.5 μm (Boord, 1969; Fischer *et al.*, 1994). In the chicken, a baso-apical gradient was found, with the largest axons apically (Fischer *et al.*, 1994). The present study was designed to gain more detailed knowledge about auditory-nerve axons in birds. The barn owl was chosen as a well-established species in auditory research, with quite detailed information available on the anatomy of the basilar papilla and its innervation (Smith, C. A., *et al.*, 1985; Fischer *et al.*, 1988; Köppl, 1993; Fischer, 1994b). In addition, the frequency map is known (Köppl *et al.*, 1993). Since we have begun recordings from the auditory nerve in the barn owl, knowledge about fibre sizes is desirable as potentially important for the interpretation of electrophysiological data. Also, any variations across frequencies might provide clues to the relative physiological importance of parameters, such as axon size and myelination, that influence conduction velocity and possibly temporal resolution (e.g., Rushton, 1951; Paintal, 1966; Smith, R. S. and Koles, 1970; Ritchie, 1982). The barn owl is especially suited to answer these questions, since it is known to encode temporal information very accurately through phase-locking of the auditory afferents up to unusually high frequencies (Sullivan and Konishi, 1984; Köppl, 1995). Another point of interest was the total number of afferents and their distribution across frequencies, which might indicate the relative importance of different frequency bands for further central processing.

Since the auditory nerve in birds carries the fibres of both the basilar papilla and the lagenar macula, a vestibular organ situated at the apical end of the cochlear duct in all non-mammals (e.g., Boord and Rasmussen, 1963; Manley *et al.*, 1991a), some basic data on lagenar macular axons are also reported. The two fibre populations cannot be sharply distinguished once the lagenar fibres have joined the cochlear ganglion and nerve. An independent analysis of the lagenar nerves only was therefore carried out, primarily to estimate their proportion of the total auditory nerve and determine their spectrum of axonal sizes.

METHODS

The results from 5 adult barn owls (*Tyto alba guttata*), aged 1–2 years, are reported in this study. They were deeply anaesthetized with overdoses of either Ketamine or Na-pentobarbital. After cessation of the breathing reflex, the animals were perfused transcardially with warm saline (0.9% NaCl with heparin added), followed by one litre of fixative. Several different mixtures of Paraformaldehyde (PFA) and

Glutaraldehyde (GA) were used as fixatives: a) 2% PFA and 2.5% GA, b) 2% PFA and 1.25% GA, c) 1% PFA and 2.5% GA, all in 0.1M phosphate buffer, pH 7.4–7.6. The fixative was either immediately followed by a buffer rinse (initial specimens plastic-embedded en bloc, see below) or the entire head was left in fixative in a refrigerator for 1–2 days. The auditory nerve and ganglion were then carefully dissected out on both sides, together with the vestibular ganglia, nerve branches and a piece of brainstem. In most cases, the lagenar end of the cochlear duct was also preserved, sometimes even the complete basilar papilla; the macular otolith was removed to facilitate sectioning later. After washing in buffer, the initial specimens were postfixed in 1% OsO_4 in phosphate buffer for 1–2 hours, washed again, then dehydrated in a graded series of alcohols and embedded in Araldite via propylenoxide.

While this technique of dehydrating and embedding en bloc gave good results for the lagenar part, serious difficulties were encountered with the auditory nerve, such that there often appeared to be a gradient of decreasing osmification and/or plastic infiltration towards the middle of this large nerve. A different procedure was therefore subsequently adopted: specimens were embedded in an albumin-gelatine mixture for either vibratome or cryostat sectioning, the latter being infiltrated with 30% sucrose beforehand, and serial sections of 100µm thickness were cut. If the basilar papilla and lagenar macula were also preserved, the most basal and most apical portions of the cochlear duct were cut off with fine iris scissors beforehand. The 3 pieces thus obtained from the same ear were then embedded separately and oriented differently for sectioning. The floating sections were examined under low magnification to select cross-sections of the auditory nerve approximately at the level where it passes through the internal auditory meatus ("central sections"), as well as cross-sections of the cochlear ganglion and, if present, the basilar papilla and macular lagena, at approximately 1mm-intervals in both directions from this central point. At each chosen location, 1 or 2 serial sections were taken, destined for later thin sectioning. The remaining sections were mounted on gelatine-coated slides, stained with neutral red and cover-slipped. These were later used to reconstruct the total extent of the basilar papilla and determine the relative positions of the semithin sections analyzed in detail.

Sections destined for thin sectioning were then postfixed in 1% OsO_4 in phosphate buffer for 2 hours on ice, washed, dehydrated in a graded series of alcohols and embedded in araldite via propylene oxide. To prevent distortion of the sections, they were restrained flat in a custom-built holder during the dehydration steps. Semi-thin and ultra-thin sections were cut mostly from such plastic-embedded thick sections, a minority from specimens plastic-embedded en bloc. Semi-thin sections were stained with 0.2% toluidin blue in 0.2% borax solution, ultra-thin sections with uranyl acetate and lead citrate.

The best semi-thin sections from each specimen were digitized via a PC framegrabber interface receiving input from a video camera attached to the microscope. Each section was stored as a series of contiguous, but non-overlapping, images by systematically stepping the field of view along and across in a grid-like fashion. Using a ×40 objective (corresponding to ×1350 magnification on the video monitor), about 50 images were necessary to cover a whole auditory nerve. For sections of the lagenar nerve bundles, a ×100 objective was used (corresponding to ×3400 magnification on the video monitor). For each image, the axon profiles (enclosed by but excluding the myelin sheath) were then defined using standard image analysis software (analySIS; Soft Imaging Software, Münster, Germany). The necessary steps involved image sharpening, contrast enhancement, definition of a window of grey values for particle detection and subsequent manual editing (examples in Figs. 1 and 2). Axons bordering the edge of the image were excluded if less than half of their profile was thought to be showing. For each particle so defined, the following automatically-measured parameters were then stored: 1. The X-and Y-coordinates of the particle's centre of gravity. 2. The diameter, derived by sliding 2 tangents around the particle in 15° steps and measuring the distance between the 2 points on the particle's outline touching the tangents; both the maximal and minimal diameter were stored. 3. The

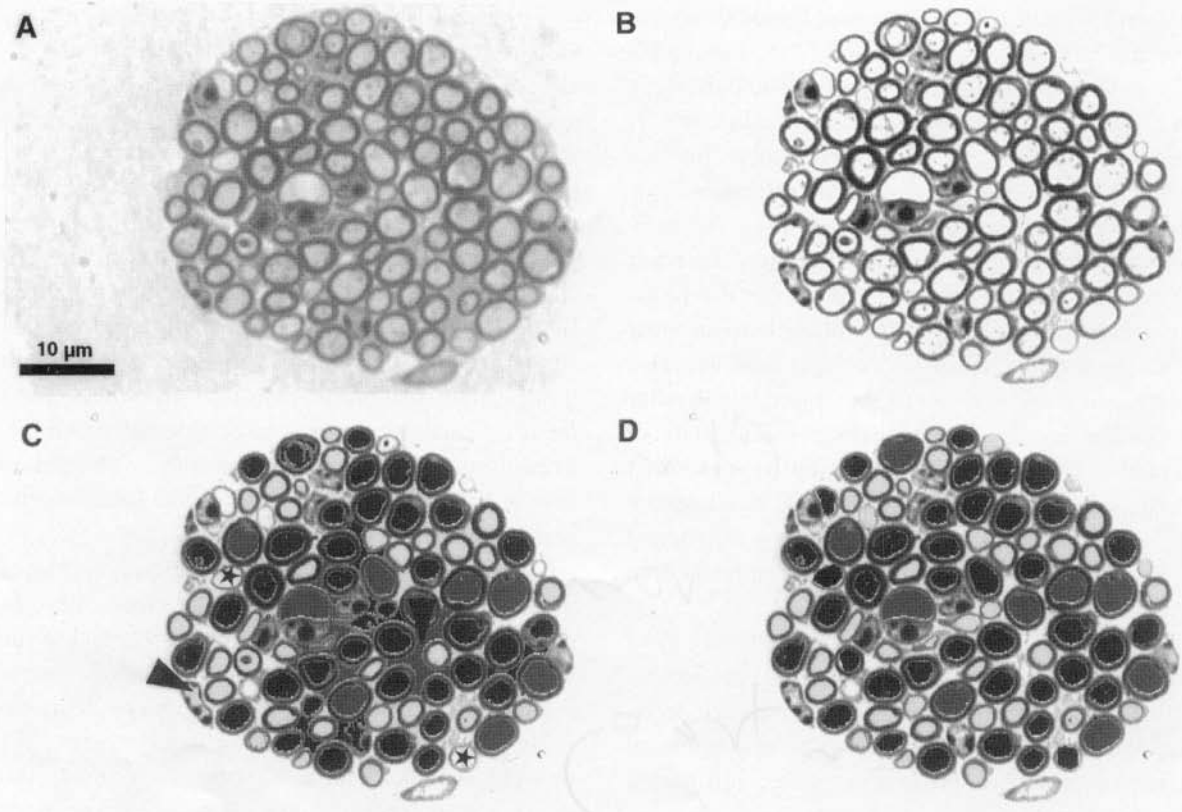

FIGURE 1 Example of the major steps of the semi-automated image analysis used to define axons in peripheral semi-thin sections that only contained lagenar fibres. Each image shows about half the area visible on the video monitor, using a ×100 objective on the microscope. **A**: Digitized microscope image. **B**: The same image as in A, but after digital sharpening and contrast enhancement. **C**: The same image as in B, with a coloured overlay, showing individual particles covering areas of a custom-defined range of grey values. The different colouring according to diameter is simply a visual aid and bears no importance for further analysis. Note some errors, i.e., particles that are not axons (two examples marked with arrowheads) and axons not detected (two examples marked with asterisks). **D**: The same image as in C, but after interactive correction of detection errors. At this stage, particle parameters were measured automatically and stored. Refer to color version at the back of the journal.

equivalent circle diameter (ECD), derived from the particle area (A), assuming a circular profile:

$$ECD = 2\sqrt{(A/\pi)}.$$

Control counts of the number of fibres were carried out manually from video-print montages of the stored images (print magnification ×500 and ×1250, respectively, depending on the objective used for recording).

Ultra-thin sections were viewed with a Jeol-100× transmission electron microscope (TEM) at 100 kV acceleration voltage. A continuous strip of photographs was taken at ×2600 magnification, covering a complete transect approximately along the midline of the short axis of the cross-section in one specimen, and at ×2000 magnification covering a transect approximately along the midline of the long axis of the section in another specimen. The photographic negatives were digitized using a flatbed scanner with a transparency adapter. Measurements were then made at a final magnification of ×7800 and ×6000 on the video monitor, respectively, using the interactive distance measuring utility of the image analysis software. Axon and fibre diameter were subjectively defined as the widest cross-sectional distance, perpendicular to the long axis. Fibre diameter was defined as including the myelin sheath, axon diameter as the corresponding distance within the myelin sheath, assuming there is

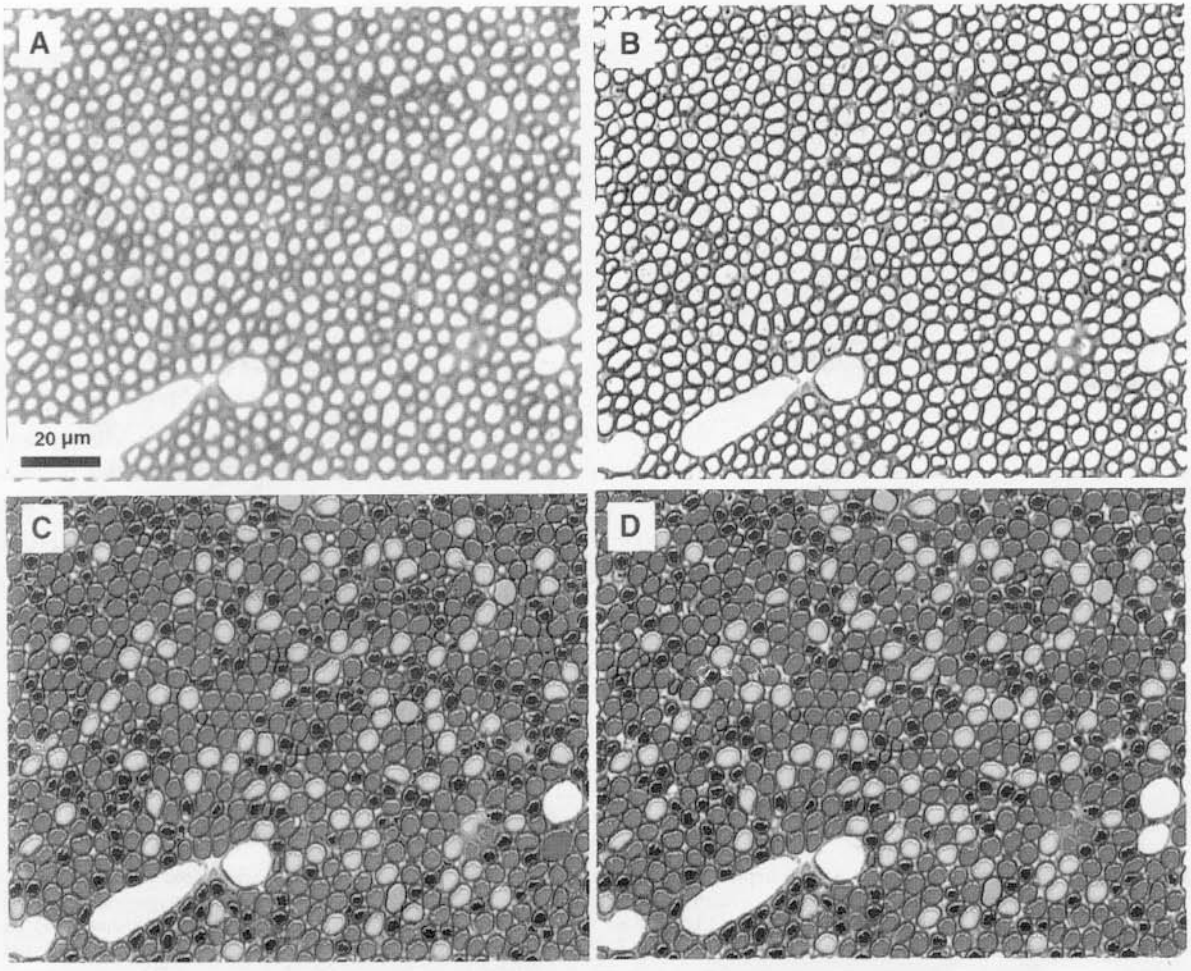

FIGURE 2 Example of the major steps of the semi-automated image analysis used to define axons in most semi-thin sections. Each image shows about half the area visible on the video monitor, using a ×40 objective on the microscope. Panel layout is the same as in Figure 1. The large objects that were left undetected are blood vessels. Refer to color version at the back of the journal.

normally no significant distance between the axon membrane and the inner-most myelin layer.

RESULTS

Distinction of Fibre Populations

Cross-sections of the auditory ganglion and nerve of the barn owl were obtained at varying levels (Fig. 3). Measurements of the whole population of fibres were derived from complete sections at a level near the internal auditory meatus where the nerve passes through the brain capsule. At this level, which will be referred to as "*central sections*" (Fig. 3) in the following, the nerve consists of both afferent and efferent fibres that supply the basilar papilla and the lagenar macula. There are therefore four basic groups of fibres: afferent-papillar, efferent-papillar, afferent-lagenar and efferent-lagenar. These four groups will also be represented at all levels that lie more apical. At locations beyond the internal auditory meatus, i.e., further towards the base of the papilla, only papillar afferents and efferents will be encountered (Fig. 3).

A distinct fibre bundle containing efferent fibres was easily identified in all central sections (Fig. 4). Evidence

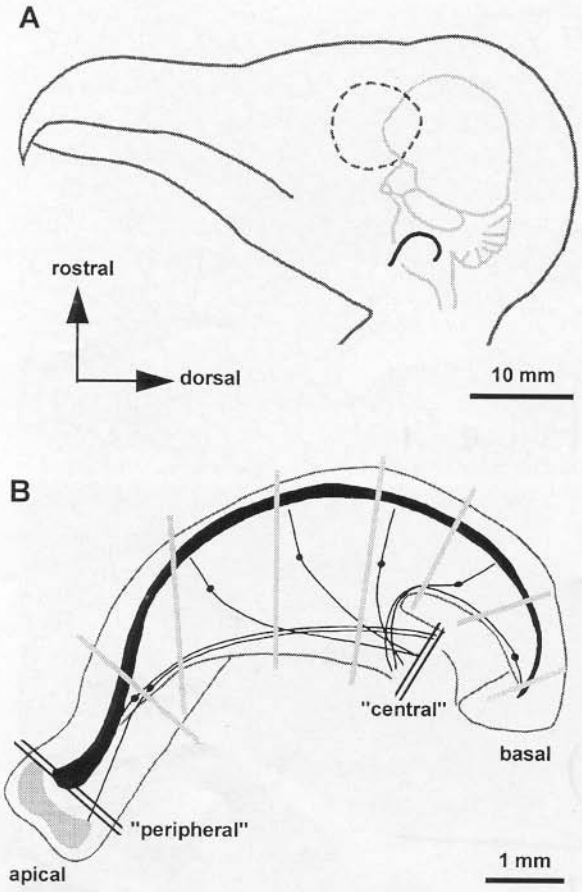

FIGURE 3A Schematic drawing of the skull of a barn owl, as seen from the left. The dashed circle indicates the location of the eye. The brain, whose long axis defines the rostrocaudal and dorsolateral axes, is drawn in light grey. The cochlear duct is indicated schematically as a black curved line adjacent to the brainstem. In B, an isolated cochlear duct is drawn at higher magnification, but with the same general orientation. Note that the curvature of the barn owl's cochlear duct is actually three-dimensional, such that the apical third would be curving away from the observer towards the skull's midline. The solid black band indicates the basilar papilla, the grey band at the very apical end shows the macular lagena. Several examples of afferent neurones, including one from the lagena, are also drawn in black, to illustrate their typical paths and the positions of their cell bodies. Black double lines indicate the levels of central and peripheral cross sections that were used for evaluation of either the complete auditory nerve or the lagenar fibres only, respectively. Thick grey lines indicate the approximate positions of several additional cross sections analyzed to differentiate between fibres of different frequency ranges.

for the efferent nature of this bundle and the characteristics of its fibres will be described as part of a separate publication (in preparation). The efferent fibre bundle could also be distinguished peripherally, running along the cochlear ganglion. Only at very apical and basal positions, respectively, where the efferent fibres dispersed and/or became very few, a reliable distinction was not possible. Unless mentioned otherwise, only results excluding the efferent bundle will be presented in this study and it will be assumed that these are all from afferent fibres.

A distinction between afferents from the basilar papilla and lagenar macula was not possible with any certainty in central sections, or in sections along the cochlear ganglion. Although the general area where the lagenar fibres clustered was easily recognized by their heterogenous axon diameters, there was no distinct border between the two populations. Only in sections cut near the apical end of the basilar papilla, which will be referred to as "*peripheral*" (Fig. 3), was the lagenar fibre population clearly separable (Fig. 5). Unfortunately, afferent and efferent lagenar fibres could not be distinguished at this peripheral level.

Accuracy of the Image Analysis Used

A semi-automated procedure of particle detection in video images was used to obtain fibre counts and measurements from complete nerve sections, avoiding introducing biases into the data by sampling. The following potential sources of deviation and/or error (compared with conventional sampling and measuring methods) have to be considered:

1. Particle detection was never perfect. An individual image could contain as many as 1,500 particles, and no matter how carefully the interactive user scrutinized the particles defined, there could be no certainty that each particle corresponded to an axon and that each axon was detected. The control counts carried out manually from videoprints were therefore compared to the particle counts derived from video analysis. For 9 individual images from central nerve sections, the ratio of particle count/hand count varied mostly between 1.015 and 1.069; in one extreme case it reached 1.231. Numbers tended to deviate more for images with small fibres and/or a loose arrangement of fibres; in the latter case, the particle count sometimes included a substantial number of inter-fibre spaces. However, images with these conditions were

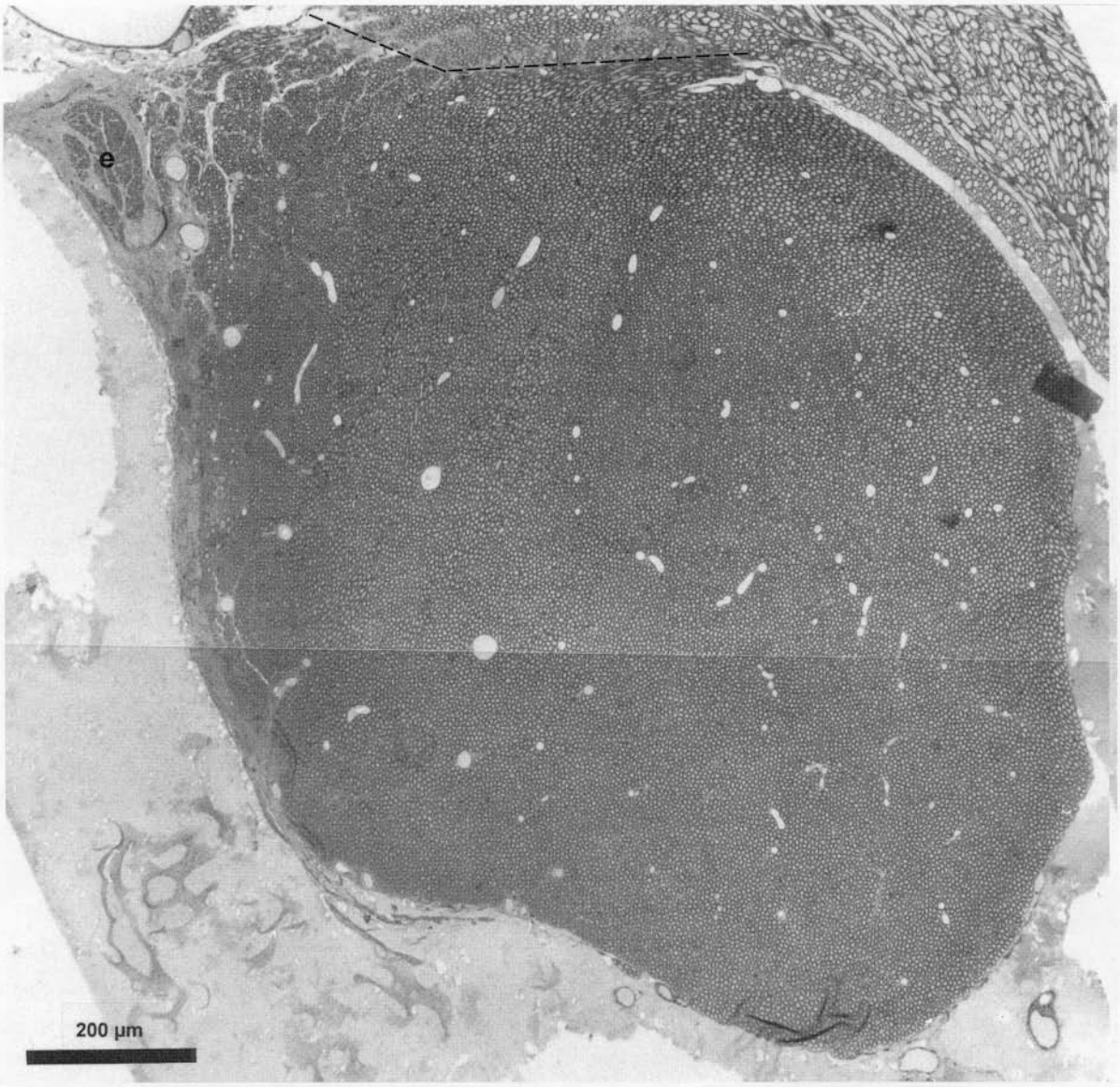

FIGURE 4 Low-magnification view of a semi-thin central section of the auditory nerve. At the top, a piece of the brainstem is also visible where the border of the auditory nerve is indicated by the dashed lines. Also note the distinct small fibre bundle marked with an "e" in its centre (top left), which was identified as efferent (see text). The dark rectangle at the right edge of the nerve is an artefact.

rare within the total number of some 50 images covering one central nerve section. Averaged over all 9 control counts, the count ratio was 1.057 (n = 9), i.e., the particle count tended to be 5.7% higher than the manual count. Since, in the peripheral sections, lagenar fibres tended to be small and loosely arranged, a higher magnification (see Methods) was used for these. Count ratios for 3 complete counts of peripheral sections varied between 1.018 and 1.070, with the particle count lying, on average, 3.6% above the manual count. It may thus be assumed that the video analysis used overestimates the number of axons by approximately 5%, chiefly due to the erroneous inclusion of non-axon particles.

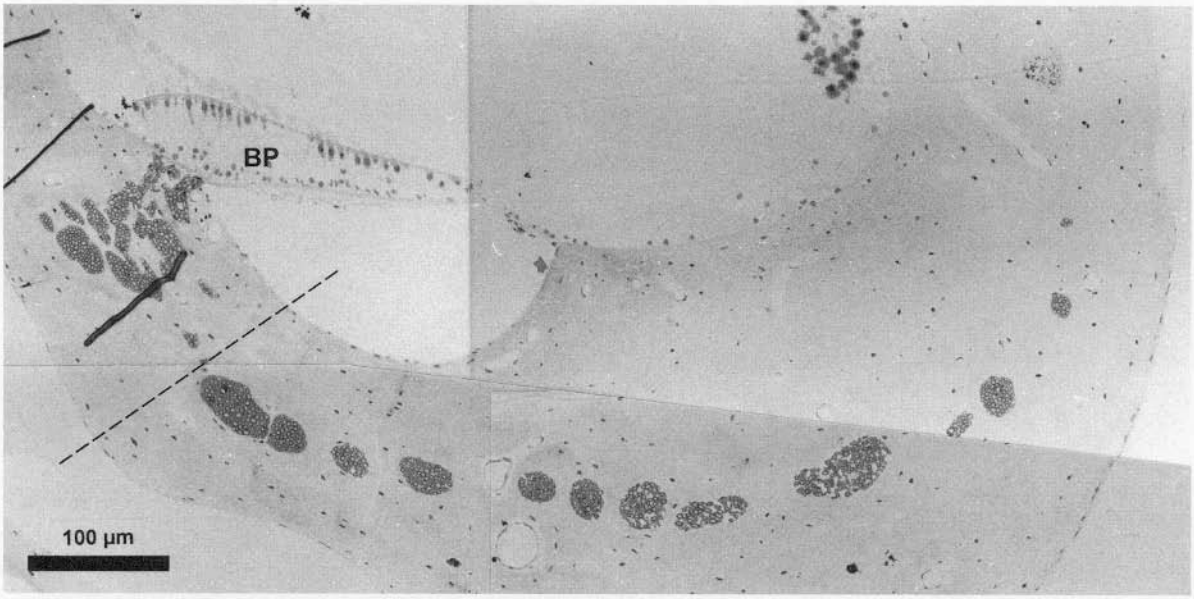

FIGURE 5 Low-magnification view of a semi-thin peripheral section near the apical end of the basilar papilla (marked "BP"). The dashed line separates the papillar fibres (to the left) from the lagenar fibres (to the right) as determined by perusal of serial sections beyond the apical end of the papilla. Note the homogenous appearance of the small group of papillar fibres in contrast to the mixed fibre sizes in the lagenar bundles. The dark bands on the left are artefacts (small folds in the section).

2. There are different methods for defining axon diameter. According to Karnes *et al.* (1977), the most accurate representation is achieved by the equivalent circle diameter (ECD, see Methods). This method, however, overestimates the axon diameter if the plane of section deviates from an ideal cross-section. Special care was therefore taken to obtain sections with a minimal number of fibres appearing to be obliquely cut. In the absence of any established criteria, we followed Arnesen and Osen (1984) and used the quotient of maximal and minimal diameter (see Methods) to assess the roundness of the particle profiles. All particles with a quotient >2.0 were discarded for axon size measurements. These were between 3.1% and 23.3% of all particles in different sections. In a small sample of fibres from TEM photographs, a subjective definition of axon diameter (the widest distance across the axon perpendicular to its long axis) was compared to the ECD and the minimal diameter as given by the image analysis. The minimal diameter corresponded very well to the subjective measurement, with an average deviation of only 5%. The ECD was, on average, 25% larger than the subjective measurement. Since similar subjective definitions were used in most of the studies published on auditory nerves, we will show data for both the ECD and the minimal diameter.

Total Number of Afferent Fibres

Three central sections from completely-preserved nerves, two of these from the left and right sides of one individual, were analyzed. The number of afferent fibres counted by image analysis varied very little, from 34,154 to 34,218 (Table I). The average number was 34,187. Subtracting 5% (the estimated error of the image analysis method used, see above), leaves an average of 32,478 papillar and lagenar afferents.

The number of lagenar fibres counted in 4 peripheral sections from different individuals varied considerably, from 1,087 to 1,710. Since one of the specimens could only be counted manually (because the contrast proved insufficient for the image analysis), manual counts only are given for all specimens (Table I). The average number of lagenar fibres was 1,342.

TABLE I Number of fibres and average axon diameter measures for 3 centrally-sectioned specimens, i.e., all afferent fibres, and 4 peripherally-sectioned specimens, i.e., lagenar fibres. Fibre numbers were determined by image analysis for the central sections and include all detected particles. For peripheral sections, only manual counts are given, because one specimen was not suitable for image analysis. Values given for axon ECD and minimal diameter were determined by image analysis in all cases and include only particles whose ratio of maximal/minimal diameter was <=2.0.

specimen	number of fibres	mean ECD ± st.dev.	mean min.diam. ± st.dev.
all afferents (central sections):			
TAE16 right	34188	2.91 ± 0.68	2.81 ± 1.10
TAE16 left	34154	2.84 ± 0.71	2.57 ± 0.71
TAE20 left	34218	3.46 ± 0.77	2.96 ± 0.76
lagenar fibres (peripheral sections):			
Tyto18 right	1710		
Tyto26 left	1110	2.07 ± 0.71	1.92 ± 0.64
Tyto29 left	1377	2.40 ± 0.88	2.18 ± 0.81
Tyto33 left	1171	2.02 ± 0.64	1.88 ± 0.59

Subtracting the average lagenar fibre count from the total afferent count leaves an average number of 31,142 papillar afferent fibres. This number includes a small uncertainty since the peripheral lagenar count included efferents, whereas the central count did not. However, the whole lagenar fibre population was such a small proportion of the total auditory-nerve fibre count in the barn owl that the potential error can be assumed to be very small and will be ignored for the purpose of the present paper.

Number of Papillar Afferents Across Frequencies

We were interested to see what proportions of the afferent fibre population derive from different regions of the basilar papilla, i.e., represent the different frequency ranges. Counts were therefore made at different positions along the basilar papilla: at 9%, 21%, 33%, 45%, 58% from the apical end of the papilla and at a central level in one ear, and at 72%, 84% and 95% from the apical end of the papilla from the other ear of the same animal (see Fig. 3). At the most apical level, papillar and lagenar fibres could be clearly distinguished; at all other levels up to 58% and centrally, the average number of 1,342 lagenar fibres was subtracted from the total count. The efferent fibre bundle could be reliably excluded between 33% and 72%, as well as in the central section. At more apical levels, there appeared to be very few efferents (own unpublished observations) and no attempt at correcting for their number was therefore made. At more basal levels, fibres running peripheral to the cochlear ganglion were excluded, since a large proportion of these appeared to be efferent (own unpublished observations). The individual counts thus derived represent the cumulative number of afferent fibres successively joining the nerve, beginning at the apical end up to 58% along the basilar papilla and, by simple subtraction from the total count, also up to the basal end (Fig. 6A). This cumulative distribution shows that the majority of afferent fibres derive from approximately the apical 60% of the basilar papilla, with a marked flattening of the curve, i.e., less growth in fibre number, in the basal 30–40%. Using the cochlear map for the barn owl (Köppl *et al.*, 1993), these positional data were also converted to frequency (Fig. 6B). Frequencies below about 2 kHz are thus seen to be underrepresented in terms of afferent fibre numbers, and higher frequencies are represented with approximately equal shares of fibres for each octave.

The counts were compared with an estimate of fibre numbers across frequencies derived from hair-cell innervational data in the barn owl (Fischer, 1994b). Using Fischer's values for the number of afferently-innervated hair cells across the width at different positions along the basilar papilla and the number of afferent terminals on each hair cell across the width, expected total numbers of afferent fibres were calculated for the different papillar regions. For the most apical region, a correction factor of 0.5 was applied, since every afferent was observed to contact an average of two hair cells there (Fischer, 1994b). Actual counts and calculated fibre numbers are compared in Figure 6 and were in excellent agreement.

Axon Diameters

Two different methods, ECD and minimal diameter, were used to measure axon diameters (see above). In central nerve sections, the average ECD was 2.91, 2.84 and 3.46 µm in 3 different specimens, respectively; the average minimal diameter was 2.81, 2.57 and 2.96 µm

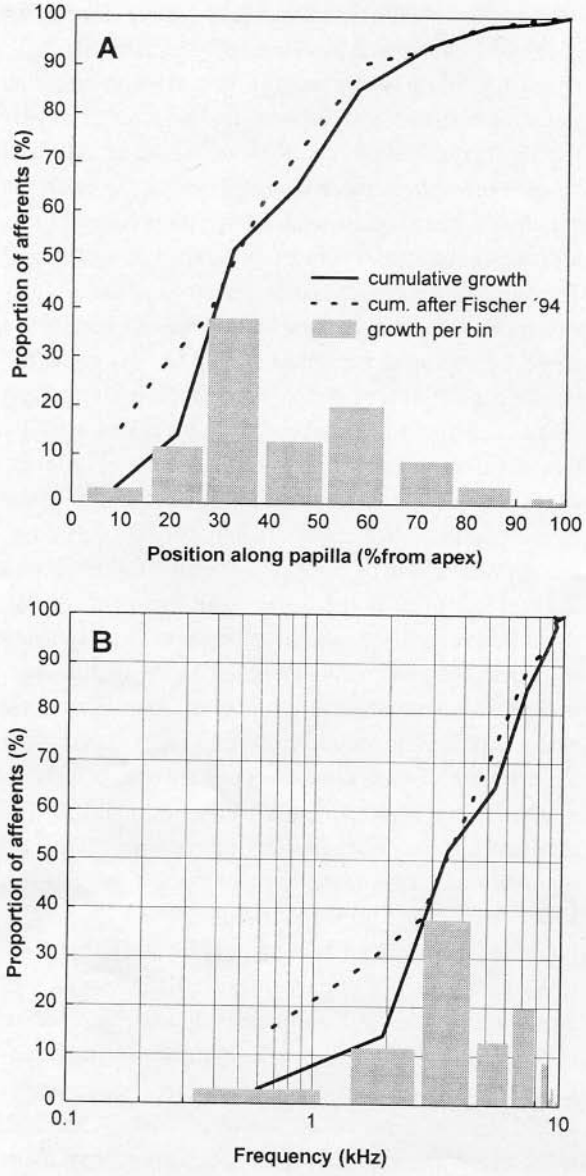

FIGURE 6 Fibre numbers from different regions of the basilar papilla, normalized to the total number of papillar fibres determined in a central section, as a function of the position along the basilar papilla (A) or the corresponding characteristic frequency (B). The solid line gives the cumulative fibre number counted in progressively more basal sections, bars show the difference between successive sections. The dashed line is an estimate of the cumulative fibre number calculated from the data given in Fischer, 1994b (see text).

(Table I). Two factors may have contributed to the variation seen between specimens, apart from differences between individual animals. First, the preparation with the largest axon diameters (TAE20) was fixed using a higher aldehyde concentration than for TAE16 (fixatives a) and b), respectively; see Methods). Second, one of the specimens (TAE16 right) was initially sectioned with a vibratom, the other 2 with a cryostat, necessitating sucrose infiltration for cryo-protection. However, this methodological difference appeared to have only a minor influence, since the 2 cryo-sectioned nerves were the ones with the smallest and largest average axon diameters, respectively.

Figure 7 a to d shows the axon size distributions for each nerve separately, as well as combined and normalized across specimens. Although extreme values ranged from 0.95 to 9.9 μm for the ECD, and from 0.75 to 13.92 μm for the minimal diameter, the great majority of axons fell between 1.0 and 5.5 μm. The distribution was thus within a narrow range and only slightly skewed towards larger values.

In two specimens, sample measurements from ultrathin TEM sections along a transect of the nerve (see Methods) each could be directly compared to light-microscopical measurements from the same areas in the neighbouring semi-thin sections. Axon diameters obtained with both techniques were virtually identical: 2.58 ± 0.77 μm (n = 1130; TEM) and 2.64 ± 0.59 μm (n = 3175; LM, minimal diameter) in one specimen; 3.05 ± 0.66 μm (n = 779; TEM) and 2.96 ± 0.79 μm (n = 939; LM) in the other specimen. Also, there was no evidence for a significant population of very small and/or unmyelinated fibres that may be missed in the light microscope (see also below under Myelination).

For lagenar axons in peripheral sections, the average ECD was 2.07, 2.40 and 2.02 μm in 3 different specimens, the average minimal diameter was 1.92, 2.18 and 1.88 μm (Table I). The ECD ranged from 0.21 to 7.17 μm, the minimal diameter from 0.32 to 8.94 μm. Lagenar axon calibres thus covered a similar range to those of the total afferent population but were much smaller on average, resulting in a more skewed distribution (Fig. 8).

One of the transects analyzed from an ultrathin central section also included a small part of the presumed lagenar fibre area. Although no sharp distinction between papillar and lagenar fibres is possible at that level, a tentative classification was made to compare the axon diameters derived from TEM measurements

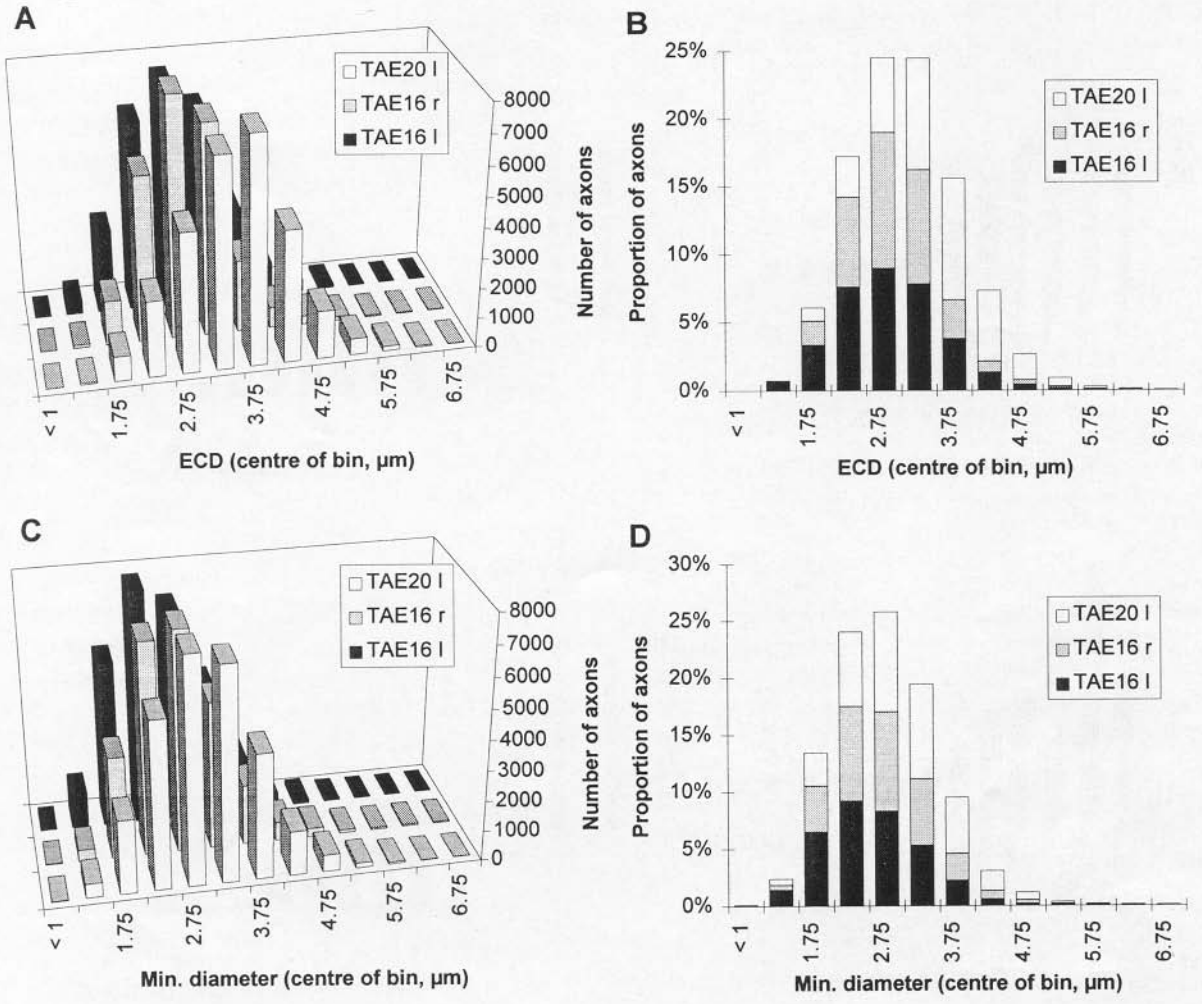

FIGURE 7 Distribution of axon sizes in central sections of the auditory nerve, classified into 0.5 µm bins, except for values below 1 µm, which were lumped since this range is at the limit of light-microscopical resolution. Distributions of the ECD (A,B) and minimal diameter (C,D) are shown for three different specimens, first separately (A, C), then cumulatively and normalized (B, D).

to those from the same area in the neighbouring semithin section. In contrast to the very similar values resulting for the papillar population with both techniques, values for the presumed lagenar fibres differed considerably: 1.50 ± 0.79 µm (n = 64; TEM) and 2.29 ± 0.80 µm (n = 55; LM, minimal diameter).

Variations in Axon Diameter with Frequency

Axon calibres were not homogeneously distributed in the barn owl's auditory nerve. A typical example of the size distribution in a central section is shown colour-coded in Figure 9. Axon calibres were smallest along the rostrolateral edge, with minimal diameter around 2 µm and ECD around 2.5 µm. A large and homogeneous population of axons with minimal diameters of 2–3 µm and ECDs of 2.5–3.5 µm made up the bulk of the nerve. The largest axons with minimal diameters of 3–4 µm and ECDs of 3.5–4.5 µm, formed a shell all along the medial edge of the nerve.

The diameter of auditory-nerve axons thus increased from rostrolateral to caudal to medial by about 2 µm. This raises the obvious question as to whether the distribution of axon sizes is correlated

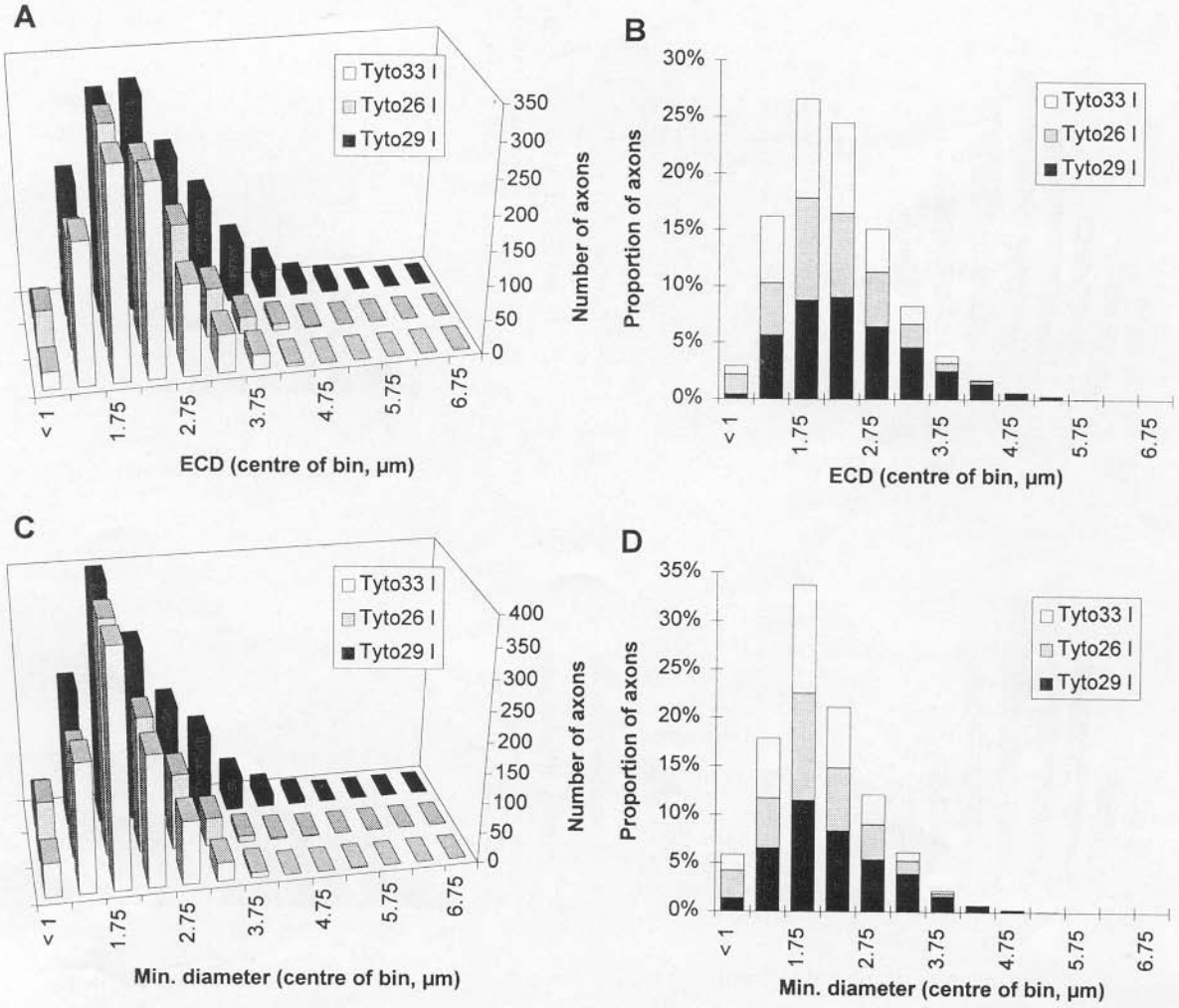

FIGURE 8 Distribution of lagenar axon sizes in peripheral sections. Panel layout is the same as described for Figure 7.

with the tonotopic organization of the nerve. However, there is no published information on the tonotopic organization of the nerve. Perusal of serial sections indicated that it is probably not constant, since the position of any given group of fibres changes along the nerve: as new fibres entered the nerve at progressively more basal locations, they appeared to join mainly at its medial edge, displacing the fibres already present from more apical locations progressively caudally and then rostrolaterally within the nerve. Subsequently, after passing through the brain capsule, the nerve appeared to spiral. These observations agree globally with descriptions of the pigeon auditory nerve (Boord and Rasmussen, 1963). It is thus difficult to determine precisely the location of axons of different frequency in any one section.

Axon sizes were therefore measured in a series of sections at different levels along the basilar papilla (as described above, see also Fig. 3). Contour plots were derived, showing the locations of various axon sizes within each section, as well as size distributions showing the difference in axon sizes from one section to the next-basal section in the series (Fig. 10). This sequence clearly documents a systematic variation of axon calibre with frequency. Axons from the most apical regions of the papilla (Fig. 10A, B), corresponding to

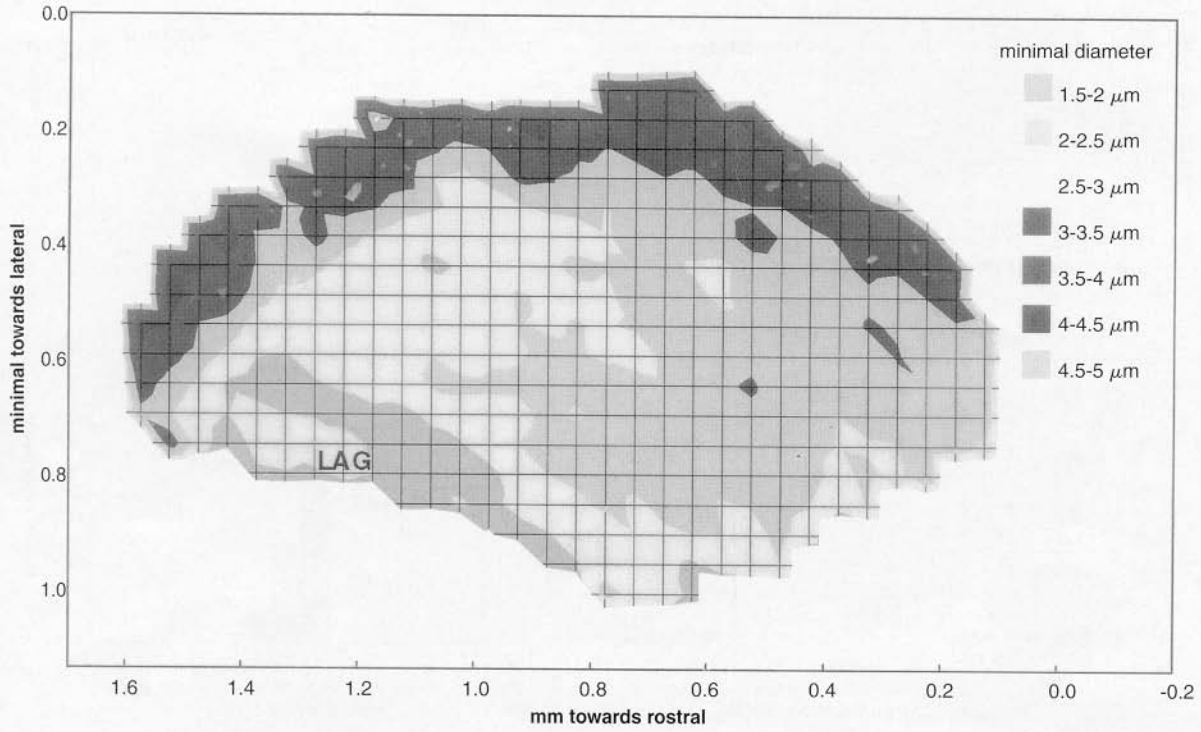

FIGURE 9 Example of the distribution of axon minimal diameters in central sections, shown as a colour-coded contour plot. The outline of the section is reproduced to scale, with the anatomical axes indicated by the ordinate and abscissa. Areas within the section are coloured according to the minimal diameter averaged over small squares of 50 × 50 μm; these squares are indicated by a fine grid, the colour code is explained in the legend (note that the red-brown areas representing diameters of 1.5–2 μm do not exactly match the brighter red in the legend). The area marked "LAG" indicates the approximate position of the lagenar fibre group. The thin halo of apparently small diameters adjacent to the large ones along the medial edge of the nerve is an artefact of the plotting procedure. Refer to color version at the back of the journal.

frequencies below 2 kHz, were generally small with minimal diameters around 2 μm and ECDs around 2.5 μm. At more basal locations, up to 45% from the papillar apex, increasingly larger axons appeared in the nerve (Fig. 10C–F). Also, the number of small axons remained nearly constant over the same distance, indicating that no great changes in the diameters of individual axons occurred. This is important because there are very few ganglion cells within the apical 15% or so, and many of the afferents measured there will have made the transition from their peripheral to their central process when measured again more basally. Using the differences between sections (Fig. 10D and F) and translating distance into frequency, axons between 2 and 3.5 kHz mostly had minimal diameters of 2–4 μm (Fig. 10D) and ECDs of 2.5–4 μm; axons between 3.5 and 5.4 kHz had minimal diameters of 2.5–4.5 μm (Fig. 10F) and ECDs of 3–5 μm. Between 45% and 58% from the papillar apex, corresponding to 5.4 to 7 kHz, very large axons around 3–5.5 μm minimal diameter (ECD 4–6.5 μm) joined the auditory nerve at its caudomedial edge (Fig. 10G, H). There was also a substantial increase in smaller axons around 2 μm diameter. However, comparing the area and location of small axons with the contour plot of the preceeding section at 45% from the apex (Fig. 10 G vs. E), the apparent increase seems to be due to a thinning of previously larger axons, perhaps related to the imminent passage of the nerve through the internal auditory meatus. This interpretation is consistent with the fact that all those small axons were missing again in a central nerve section of the same ear, close to the brainstem, as evident in the difference plot shown in Figure 10I. Up to 58% from the papillar apex or up to about 7 kHz, axons

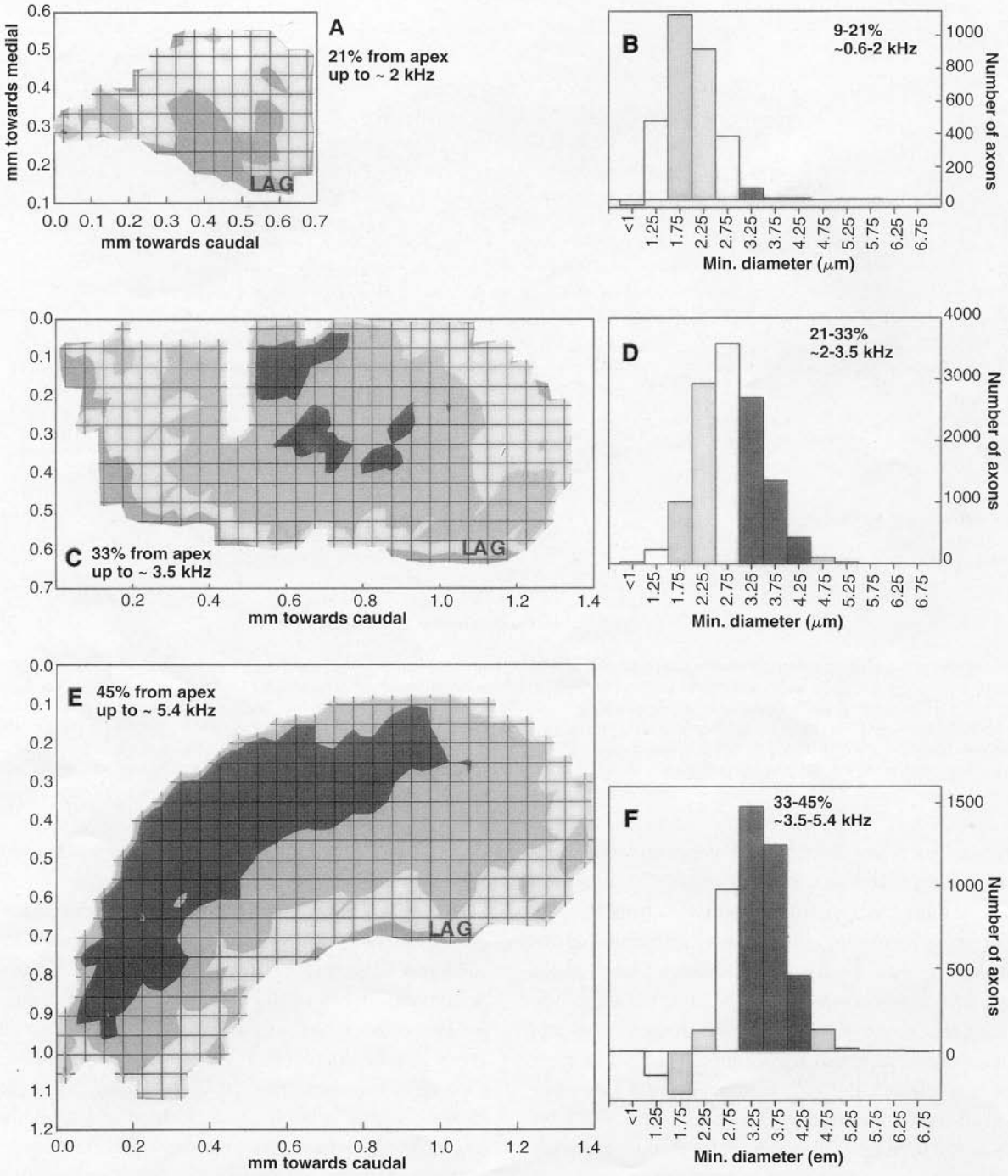

FIGURE 10 Distributions of axon minimal diameters in a series of sections from the apex to the base of the basilar papilla and nerve as indicated in Figure 3. Panels A, C, E, G and J are contour plots with the same layout and the same colour code as Figure 9. All contour plots are drawn to the same scale and are oriented alike. Panels B, D, F, H, I and K show the differences in the distributions of minimal diameters between successive sections whose position and approximate frequency range are indicated. Their bin classification and colour code also correspond to the legend in Figure 9 (note that the bright red of the bars representing diameters of 1.5–2 μm does not exactly match the more brownish red of the corresponding areas in the contour plots); bins shown in white are not represented in the contour plots if the corresponding axons were at the edge of the nerve. Refer to color version at the back of the journal.

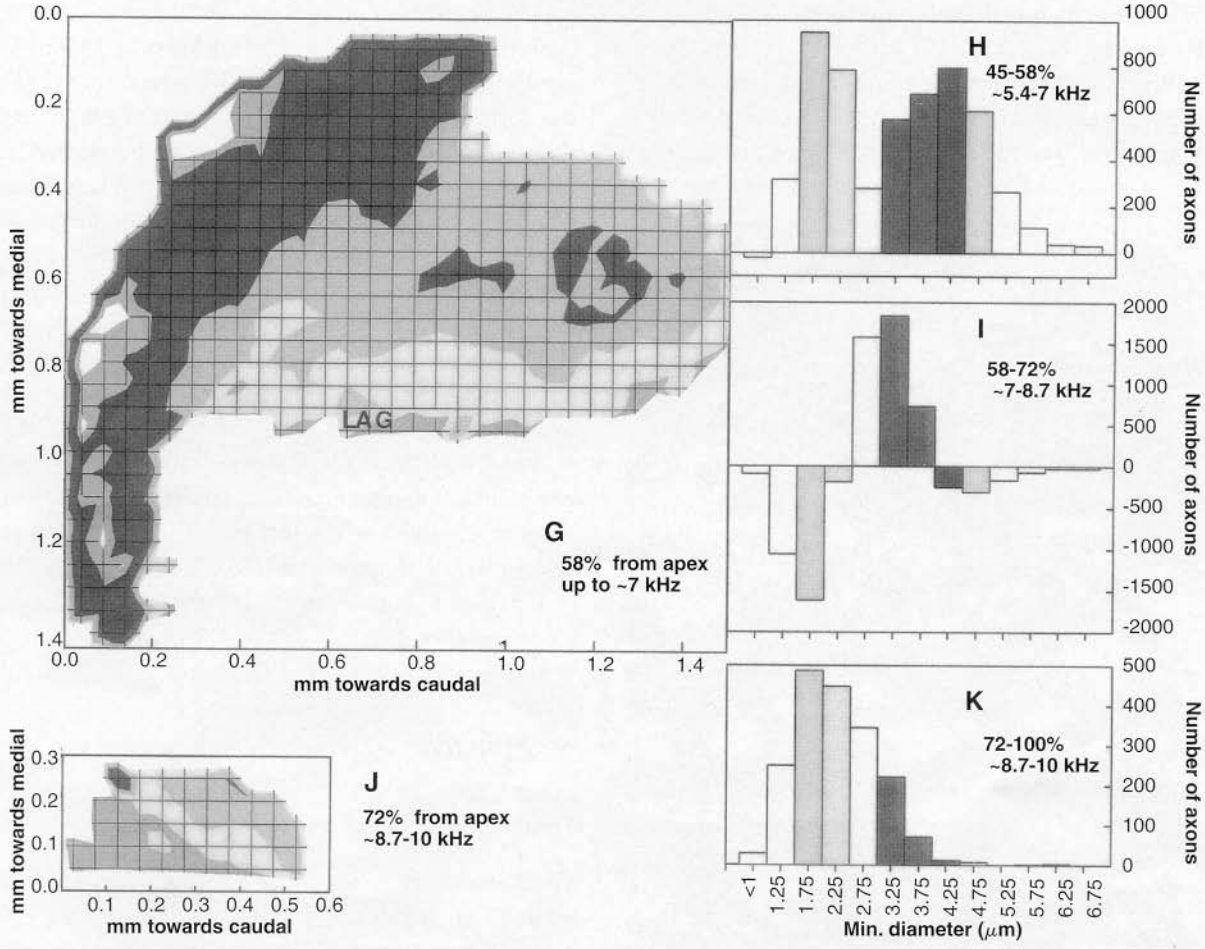

FIGURE 10 (*Continued*)

newly joining the nerve were thus of increasingly large diameter with increasing frequency. Basal to that, i.e., for frequencies higher than 7 kHz, this trend reversed. Axons with frequencies between 7 and 8.7 kHz (estimated by subtracting the values of both the 58% and 72% location from those of a central nerve section of the same ear; Fig. 10I), had a minimal diameter of 2.5–4 μm and an ECD of 3–4.5 μm. At a location 72% from the papillar apex, representing axons from the most basal 28% of the basilar papilla and frequencies above 8.7 kHz, diameters were mostly even smaller, although somewhat heterogenous (Fig. 10J, K). Sections analyzed at 84% and 95% from the apex (not shown) indicated a continuous decrease of axon diameters within this group towards the basal end, i.e., towards the highest frequencies near 10 kHz. At 95%, the average minimal diameter was down to 1.9 μm, the average ECD to 2.0 μm.

Myelination

The myelination of afferent fibres was determined from ultrathin sections, sampling a total of 1,973 fibres along two transects in two different nerves (see Methods). The transects were chosen to cross known gradients of axon size and frequency. One of them also included a small part of the presumed lagenar fibre area. Although no confident distinction between papillar and lagenar fibres is possible at that level, a tentative border was defined, segregating a sample of 64 presumed lagenar

fibres. Examples of both populations are shown in Figure 11.

Virtually all the fibres were myelinated. Unmyelinated axons amounted to no more than 1% of the total number. Myelination was very uniform across the papillar fibre population, with an average myelin thickness of 0.58 ± 0.09 µm. Assuming an average thickness of 15 nm per myelin turn (Roth and Bruns, 1993; Fischer *et al.*, 1994), this corresponds to 39 layers of compact myelin. There was no indication of any systematic variation in myelin thickness with axon diameter, except that at very small diameters below about 2 µm, the scatter increased towards lower values for the myelin sheath (Fig. 12A). The quotient of axon diameter and fibre diameter (including the myelin sheath), called the g ratio, and commonly used as an indicator of relative myelination, fell systematically with fibre diameter. This change was well described by a logarithmic relationship (Fig. 12B).

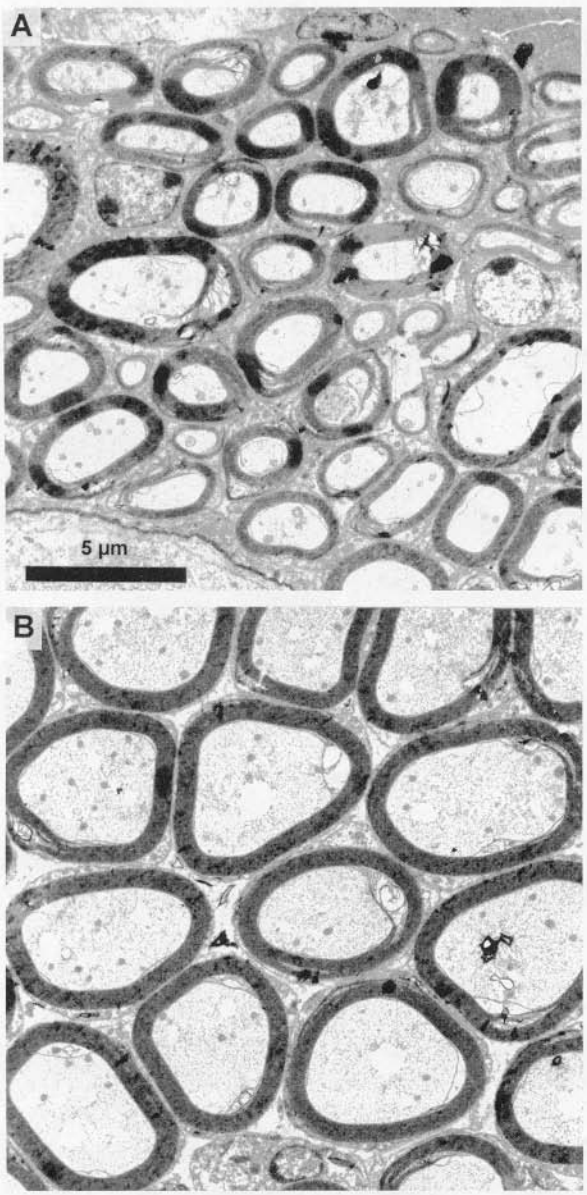

FIGURE 11 Examples of presumed lagenar fibres (A) and papillar fibres (B), as they appeared in the TEM. Both panels are shown at the same magnification. Note the heterogeneity in axon diameters as well as myelination in the lagenar population compared with the papillar one.

Presumed lagenar fibres showed more variation and generally had thinner myelin sheaths (Fig. 12A). Their mean myelin thickness was 0.39 ± 0.15 µm. This was also reflected in their g ratios, which generally lay above those of papillar fibres and showed no discernable trend (Fig. 12B).

DISCUSSION

Total Number of Fibres

There are presently few studies giving counts or estimates of the number of papillar and lagenar fibres in avian auditory nerves. It appears that, generally, the number of lagenar fibres varies far less between species than that of papillar fibres. Boord (1969) gave a total count of 850 lagenar fibres in the pigeon; Fischer *et al.* (1994) estimated 1,200–2,000 lagenar fibres for the chicken. This range also encompasses our average number of 1,342 lagenar fibres in the barn owl. About 1,000 fibres may thus be assumed as a reasonable estimate for the innervation of the lagenar macula in birds.

Papillar, or combined papillar/lagenar fibre numbers vary significantly between species and, unfortunately, also between different studies on the same species. It may be assumed that this is partly due to different methods of sampling. For example, the number of 32,478 papillar and lagenar afferents found in the present study is very much at variance with Winter's (1963) count of 16,550 ganglion cells in the

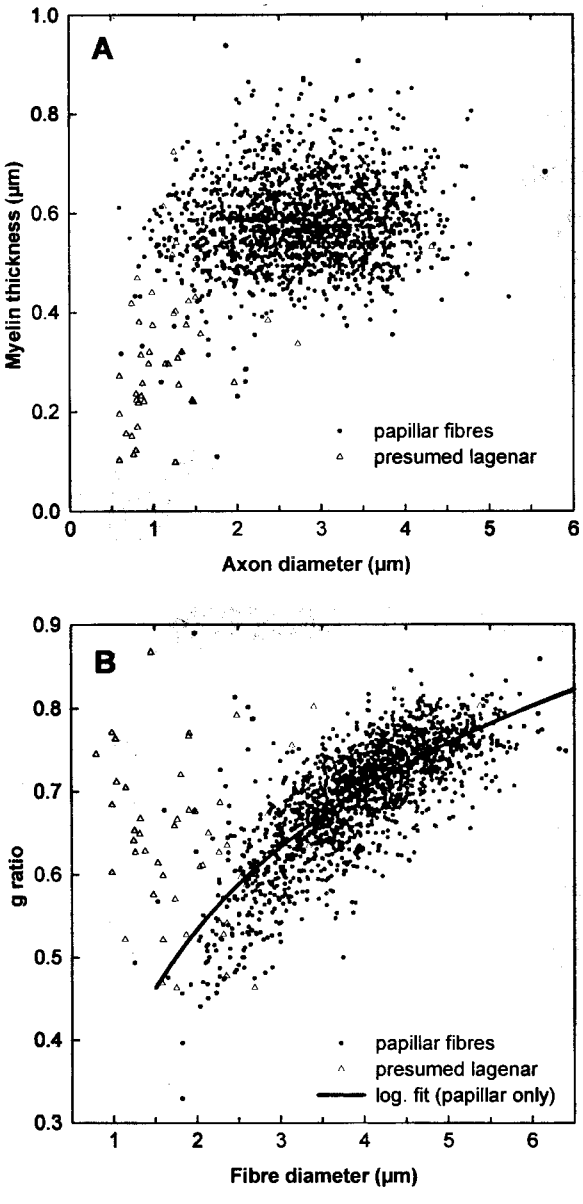

FIGURE 12 Myelination of axons in central nerve sections. Values for papillar and presumed lagenar fibres are shown using different symbols. A: Thickness of the myelin sheath as a function of axon diameter. B: g ratio (axon diameter/fibre diameter including myelin) as a function of fibre diameter. The solid line is a logarithmic fit to the papillar values only ($g = 0.364 + 0.245 \ln(\text{fibre diam.})$).

barn owl. Since we are confident about the identification of the auditory nerve, it is suggested that the method of counting cell nucleoli in thick serial sections, as used by Winter (1963), produced a large cumulative error. Our high number is also supported by Fischer's (1994b) estimate of 30,000 afferent papillar fibres in the barn owl, calculated on the basis of sample counts of the synaptic terminals on hair cells.

Assuming our average count of 31,142 papillar afferent fibres is correct, it is an extraordinary number for a bird. The chicken probably has somewhere between 8,000 (Fischer *et al.*, 1994) and 13,000 (Düring *et al.*, 1985) papillar fibres; numbers for the pigeon vary between 5,136 (Boord, 1969) and about 10,500 (Winter, 1963; subtracting 1,000 to account for the lagena). Winter (1963) also lists several other non-owl species, with cochlear ganglion cell numbers between about 5,100 and 10,700 (always subtracting 1,000 to account for the lagena). Even when the relatively large number of hair cells in the barn owl is considered, their nerve-fibre supply stands out as unusually high, as illustrated by the quotient of fibres/hair cells. For the owl, this quotient is 1.91 (31,142/16,300; Fischer *et al.*, 1988), for the chicken 0.62–1.17 (8,000–13,000/10,500–11,100; Düring *et al.*, 1985; Tilney and Tilney, 1986; Fischer *et al.*, 1994; Manley *et al.*, 1996), for the pigeon 0.53 to 1.09 (5,136 or 10,500/9,610; Winter, 1963; Boord, 1969; Gleich and Manley, 1988), and for the starling about 1.05 (6,000–6,400/5,900; Winter, 1963; Düring *et al.*, 1985; Gleich and Manley, 1988). Where ultrastructural data about hair-cell innervation are available, they confirm the trend outlined by these quotients. In chickens and starlings, those hair cells that are afferently innervated receive 1–3 fibres each, whereas in the barn owl, up to 20 afferents may contact one hair cell (Fischer, 1994a).

Afferent Innervation Density Across Frequencies

Afferent innervation density can be expressed as the number of fibres either per innervated hair cell or per unit length of basilar papilla or per frequency range. The number of afferent fibres contacting individual hair cells has been well documented through reconstructions from serial ultrathin sections in several bird species (review in Fischer, 1994a). In contrast to mammals, however, where the density of inner hair cells

does not vary much along the cochlea (e.g., Bruns and Schmieszek, 1980; Bohne *et al.*, 1982; Burda *et al.*, 1988; Spoendlin and Schrott, 1989), these data do not easily predict the number of fibres supplying different regions along the basilar papilla in birds. Hair-cell numbers per unit length of papilla vary considerably in birds, as does the proportion of afferently-innervated hair cells (reviews in Manley, 1990; Fischer, 1994a). The afferent fibre counts presented here for different regions along the basilar papilla of the barn owl therefore show the highest innervation density considerably more apical than the maximum in the number of fibres contacting a single hair cell (Fischer, 1994b). If all relevant parameters are known for a given species, however, the afferent number for entire regions of papilla can be predicted fairly accurately from ultrastructural data, as the comparison in Figure 6 demonstrates. The main discrepancy between the actual count and the calculated number was seen towards the apex, where branching of afferent fibres, supplying more than one hair cell, is known to occur (Fischer, 1994b). It is possible that the degree of branching was underestimated due to the necessarily small sample size in ultrastructural studies, leading to a corresponding overestimate of afferent fibre numbers.

In the barn owl, the apical 20% of the basilar papilla, corresponding to frequencies below 2 kHz, are underrepresented in terms of afferent fibre numbers; only 14% of all afferents derived from these cochlear regions. This distribution resembles, but does not mirror, the space devoted to different frequency bands. According to the cochlear map of the barn owl (Köppl *et al.*, 1993), higher octaves occupy a rapidly increasing amount of space, culminating in an "auditory fovea" for about 5–10 kHz, whereas afferent fibre numbers per octave plateaued at about 2 kHz. This appears to be in contrast to some bats that show similar expansions in their spatial frequency representation but, in addition, match these with regions of maximal afferent innervation density (Vater *et al.*, 1985). However, the barn owl also shows the highest density of afferent fibres per innervated hair cell in the foveal region of its cochlear map (Fischer, 1994b); only increasing numbers of afferently-innervated hair cells towards the apex result in a mismatch between spatial representation of different frequency bands and their representation in terms of afferent fibre numbers. This mismatch is significant because it suggests that the relative importance of different frequency bands in subsequent central processing is not a simple reflection of the cochlear map.

The particular pattern of innervation density along the basilar papilla of the owl, with its emphasis on frequencies above 2 kHz, is likely to be unique among birds, although few comparative data from other species exist. In the pigeon, Takasaka and Smith (1971) showed that the afferent fibre numbers per unit length of basilar papilla mirrored the corresponding hair-cell numbers, i.e., declined almost monotonically from apical to basal. According to the frequency map for the pigeon cochlea (Smolders *et al.*, 1995), an overwhelming majority (about 80%) of all afferent fibres would then derive from regions of the papilla devoted to frequencies below 1 kHz. Fischer *et al.* (1994) gave estimated cumulative fibre numbers for the chicken, calculated from samples at several points along the cochlear ganglion. Their numbers indicate a local maximum of afferent fibres at 60–70% from the apex, corresponding to about 1–3 kHz (Manley *et al.*, 1987; Chen *et al.*, 1994).

Average Axon Diameters

Both papillar and lagenar axons are larger in the barn owl than previously reported for birds. However, the discrepancy is much greater for the papillar axons.

Fischer *et al.* (1994) reported an average diameter of 1.41 μm for myelinated lagenar axons. Boord (1969) measured fibre diameters (presumably including the myelin sheath) in the pigeon, however, he only gave the size distribution, without any average values. Estimating from the distributions he gave, lagenar fibres had an average diameter of about 1.5 μm. Both these values are close to the modal values of axon diameters reported for other vestibular nerve branches in the pigeon (1–2 μm), but smaller than the average diameters of most of these (1.4 to 3.5 μm; Landolt *et al.*, 1972). This reflects the more symmetrical distribution of axon diameters in lagenar fibres (Fischer *et al.*, 1994; this study) compared to other vestibular nerve branches, which show strongly positively-skewed distributions

(Landolt *et al.*, 1972). The average diameters found for barn owl lagenar axons (around 2 μm, Table I) suggest that barn owl vestibular fibres may be generally 25–30% larger than in the chicken and pigeon.

Papillar axons in the chicken and pigeon were found to be of a similar calibre to the lagenar axons: 1.36 μm on average in the chicken (Fischer *et al.*, 1994), about 1.7 μm for fibres (presumably including the myelin sheath) in the pigeon (Boord, 1969). This is certainly not true for the barn owl. Papillar axons were both considerably larger than lagenar axons and had almost twice the diameter of papillar axons in the chicken and pigeon. The variation of axon diameters across frequency suggests that this difference in average diameters may be partly due to exceptionally high numbers of the large mid- to high-frequency fibres in the owl. However, too little is presently known about the distribution of fibre numbers and diameters across frequency in other bird species.

Owl papillar axons were close in size to myelinated cochlear axons in mammals, e.g., cat (2.8 to 3.6 μm; Gacek and Rasmussen, 1961; Arnesen and Osen, 1978), rat (2.7 μm; EL Barbary, 1991) and guinea pig (around 3 μm; Gacek and Rasmussen, 1961; Friede, 1984; Gleich and Wilson, 1993). Comparing a range of mammalian species, however, a proportional relationship between general body size and axon diameters in the auditory nerve is evident. In the mouse, cochlear axons measure only 0.8 to 2.2 μm across (Anniko and Arnesen, 1988), whereas in some whale species, average diameters are around 10 μm (Guofu and Kaiya, 1990). Considering the larger size of lagenar axons in the owl compared with other birds, part of the difference between the papillar populations may therefore also be related to the relatively large body size of the barn owl.

Variation of Axon Diameter Across Frequencies

Axon diameters in the auditory nerve of the barn owl were shown to be systematically related to the frequency range coded by different afferents. Although the method used for documenting this was somewhat indirect, relying on differences between successive cumulative fibre populations, we believe it may better reflect functionally-relevant differences than the obvious alternative, which would be measurements from tangential sections along the *Habenula perforata*. First, in mammals, axon diameters along the peripheral process of the afferent neurone have been shown to be generally much smaller than along the central process and the relationship between the two is not necessarily uniform (Spoendlin and Schrott, 1989; Ryugo, 1992). Second, in birds also, the central process is the much longer one and can therefore be expected to dominate the electrophysiological characteristics of the neurone.

The variation in axon diameter found in the owl was such that diameter first increased with increasing frequency, from about 2 μm to 4–5 μm at 7 kHz, and subsequently decreased again to about 2 μm at the highest frequencies. This trend is suited to maximize latency differences at the cochlear nucleus that are due to conduction time: apical, low-frequency afferents that have the longest travel distance between their peripheral innervation site and the brainstem have the smallest axons. Afferents at 6–8 kHz, whose peripheral innervation sites are very close to the internal auditory meatus, have the largest axons and axons get smaller again with increasing distance towards the basal end. A crude calculation of spike travel times based on standard conduction velocities of myelinated axons of different diameter (Ritchie, 1982) and estimated travel distances to the brainstem (Köppl *et al.*, 1993) predicts about 1 msec for the most apical fibres of 2 μm diameter (conducting at 10m/s over a distance of 10 mm), about 0.3 msec for fibres of 4 μm diameter (at a velocity of 20m/s over 6 mm), and about 0.8 msec for the most basal fibres of 2 μm diameter over 8 mm. Maximal differences in arrival time due to axonal travel times thus amount to about 0.7 msec, but the trend would be nonlinear across frequencies with the minimum at about 7 kHz. These latencies would combine with other known delays that increase towards low frequencies by at least one msec, such as mechanical travel times and/or differential filter response times in the cochlea (Gummer *et al.*, 1987; Gleich and Narins, 1988). The combination might result in an equalization of overall delay times for the high frequencies if the absolute values of cochlear and conduction delays match inversely.

However, no reliable estimates of these values are presently possible, since there are no data on cochlear delays in the barn owl and the calculations of axonal conduction times are based on questionable assumptions (see Discussion on Myelination below). Whether potential differences in arrival time of different frequencies in the cochlear nucleus have any physiological significance is unclear in any case. According to the stereausis model of Shamma (1989), the detection of interaural time differences could be based on differences in arrival time of different frequencies. Should a delay equalization at high frequencies exist, however, this mechanism would not work. Also, while the barn owl is known to perform interaural comparisons of ongoing time differences in the microsecond range, this kind of analysis is done separately in each frequency band at the level of the brainstem nucleus lamminaris (e.g., Carr and Konishi, 1990). Convergence of frequencies occurs later, at the level of the midbrain, after interaural time differences have been spike encoded (e.g., Takahashi and Konishi, 1986).

Friede (1984) found a similar difference in axon diameters in the guinea pig to the one described here for the owl. Afferent axons from the apical parts of the cochlea had diameters about 2 μm smaller than those from basal regions. He suggested that larger axons may rather be an adaptation to improve time signalling at higher frequencies, since there is evidence that with increasing conduction velocity, the time course of the action potential may also speed up (Paintal, 1966, 1967). This is an especially attractive hypothesis for the barn owl, since auditory-nerve fibres in this animal are known to phase-lock up to extremely high frequencies of about 9 kHz (Sullivan and Konishi, 1984; Köppl, 1995). Phase-locking is defined relative to the cycle period of the stimulating frequency, therefore the temporal precision required on an absolute scale is increasing at higher frequencies.

There is also evidence for exactly the opposite trend, i.e., smaller axons in high-frequency afferents, from a number of other species, including birds (Takasaka and Smith, 1971; Fischer *et al.*, 1994), mammals (Arnesen and Osen, 1978; Anniko and Arnesen, 1988), lizards (Miller, 1985; Mulroy and Oblak, 1985) and a frog (Simmons and Narins, 1995). Given the diversity in hearing organs of all these species, and the existence of opposing patterns of axon size and frequency, a uniform adaptive value of these patterns is not likely.

Myelination

In the present study, almost all axons were found to be myelinated, with only a negligible number of maximally 1% being unmyelinated in central nerve sections. The most likely origins of these unmyelinated axons are either autonomic fibres or efferent fibres running distributed within the nerve and not within the clearly recognizable bundle that was excluded from analysis. There is no evidence that distinct populations of afferents, like the type I and type II afferents in mammals (e.g., Ryugo, 1992), exist in birds. Spiking, spontaneously-active afferents responding to sound have been traced within the known or estimated limits of afferent innervation in the basilar papilla (Gleich, 1989; Manley *et al.*, 1989; Smolders *et al.*, 1995). Afferent terminals (e.g., Takasaka and Smith, 1971; Fischer, 1994a) and probably also cochlear ganglion cells (Fischer *et al.*, 1994) are of a uniform morphological type.

Myelinated axons were surrounded by compact myelin. The absolute thickness of the myelin sheath was found to be invariant with axon diameter for papillar afferents in the barn owl. This resembles similar measurements in the chicken (Fischer *et al.*, 1994) and the rat (Roth and Bruns, 1993). In the cat, a weak correlation was described with axon circumference, such that larger axons had thicker myelin sheaths (Arnesen and Osen, 1978). A weak, or even no, dependence on axon size means the g ratio, i.e., the relative degree of myelination, changes with both axon and fibre size. Auditory-nerve fibres thus generally do not appear to follow the rule of optimal myelination derived from other peripheral nerves, where myelination was found to be adjusted to a uniform g ratio of 0.6 to 0.7. This is a range where, theoretically, maximal conduction velocity is achieved independent of total fibre diameter (e.g., Rushton, 1951; Goldman and Albus, 1968; Smith, R. S. and Koles, 1970; Waxman and Bennett, 1972). According to this rule, many large axons in the barn owl are "undermyelinated", whereas the smallest axons are

uneconomically "overmyelinated" to gain little additional speed. This suggests that either crucial underlying assumptions, such as the proportionality of fibre diameter and internodal spacing (Rushton, 1951; Goldman and Albus, 1968), may not be valid for the auditory nerve or that economical maximization of conduction velocity is not always of primary importance.

Myelin thickness varies considerably between species. Values for the barn owl, the rat (EL Barbary, 1991) and the guinea pig (estimated from the diameters and mean g ratio given by Friede (1984) are similar, at around 0.5–0.6 μm. Chicken papillar fibres, however, have thinner myelin sheaths of only around 0.3 μm (Eisensamer, 1991) and cat fibres are thickly myelinated by 40–70 layers (Arnesen and Osen, 1978), translating into about 0.8 μm. These numbers suggest a crude correlation with general body size, as already pointed out for the average axon diameters (see above). Larger animals generally have larger axons and/or heavier myelination, possibly to compensate for their generally longer distances between the cochlea and brainstem.

Acknowledgments

I am indebted to Andrea Wegscheider for excellent technical assistance with histology and sectioning. Thanks to Franz Peter Fischer and Susanne Daum for giving valuable advice regarding ultrathin sectioning and electron microscopy; Franz Peter Fischer also generously provided numerical data from published figures. Further thanks to Geoff Manley for continuous support and discussion. This research was funded by the Deutsche Forschungsgemeinschaft through the SFB 204 "Gehör" and by a DFG fellowship.

References

Anniko, M. and Arnesen, A. R. (1988) Cochlear nerve topography and fiber spectrum in the pigmented mouse, *Arch. Otolaryngol.*, **245**, 155–159.

Arnesen, A. R. and Osen, K. K. (1978) The cochlear nerve in the cat: Topography, cochleotopy and fiber spectrum, *J. Comp. Neurol.*, **178**, 661–678.

Arnesen, A. R. and Osen, K. K. (1984) Fibre population of the vestibulocochlear anastomosis in the cat, *Acta Otolaryngol. (Stockh.)*, **98**, 255–269.

Bohne, B. A., Kenworthy, A. and Carr, C. D. (1982) Density of myelinated nerve fibers in the chinchilla cochlea, *J. Acoust. Soc. Am.*, **72**, 102–107.

Boord, R. L. (1969) The anatomy of the avian auditory system, *Ann. N.Y. Acad. Sci.*, **169**, 186–198.

Boord, R. L. and Rasmussen, G. L. (1963) Projection of the cochlear and lagenar nerves on the cochlear nuclei of the pigeon, *J. Comp. Neurol.*, **120**, 463–473.

Bruns, V. and Schmieszek, E. (1980) Cochlear innervation in the greater horseshoe bat: demonstration of an acoustic fovea, *Hear. Res.*, **3**, 27–43.

Burda, H., Ballast, L. and Bruns, V. (1988) Cochlea in old world mice and rats (Muridae), *J. Morphol.*, **198**, 269–285.

Carr, C. E. and Boudreau, R. E. (1991) Central projections of auditory nerve fibers in the barn owl, *J. Comp. Neurol.*, **314**, 306–318.

Carr, C. E. and Konishi, M. (1990) A circuit for detection of interaural time differences in the brain stem of the barn owl, *J. Neurosci.*, **10**, 3227–3246.

Chen, L., Salvi, R. and Shero, M. (1994) Cochlear frequency-place map in adult chickens: Intracellular biocytin labeling, *Hear. Res.*, **81**, 130–136.

Düring, M. von, Andres, K. H. and Simon, K. (1985) The comparative anatomy of the basilar papillae in birds, *Fortschritte der Zoologie*, **30**, 681–685.

Eisensamer, B. (1991) Die Struktur des cochleären und lagenären Innenohrganglions beim einwöchigen Hühnerküken. Diplom thesis, Lehrstuhl für Zoologie, Technische Universität München.

EL Barbary, A. (1991) Auditory nerve of the normal and jaundiced rat. I. Spontaneous discharge rate and cochlear nerve histology, *Hear. Res.*, **54**, 75–90.

Fermin, C. D. and Cohen, G. M. (1984) Development of the embryonic chick's statoacoustic ganglion, *Acta Otolaryngol. (Stockh.)*, **98**, 42–52.

Fischer, F. P. (1994a) General pattern and morphological specializations of the avian cochlea, *Scanning Microsc.*, **8**, 351–364.

Fischer, F. P. (1994b) Quantitative TEM analysis of the barn owl basilar papilla, *Hear. Res.*, **73**, 1–15.

Fischer, F. P., Köppl, C. and Manley, G. A. (1988) The basilar papilla of the barn owl *Tyto alba*: A quantitative morphological SEM analysis, *Hear. Res.*, **34**, 87–102.

Fischer, F. P., Eisensamer, B. and Manley, G. A. (1994) Cochlear and lagenar ganglia of the chicken, *J. Morphol.*, **220**, 71–83.

Friede, R. L. (1984) Cochlear axon calibres are adjusted to characteristic frequencies, *J. Neurol. Sci.*, **66**, 193–200.

Gacek, R. R. and Rasmussen, G. L. (1961) Fiber analysis of the statoacoustic nerve of guinea pig, cat, and monkey, *Anat. Rec.*, **139**, 455–463.

Gleich, O. (1989) Auditory primary afferents in the starling: Correlation of function and morphology, *Hear. Res.*, **37**, 255–267.

Gleich, O. and Manley, G. A. (1988) Quantitative morphological analysis of the sensory epithelium of the starling and pigeon basilar papilla, *Hear. Res.*, **34**, 69–85.

Gleich, O. and Narins, P. M. (1988) The phase response of primary auditory afferents in a songbird (*Sturnus vulgaris L.*), *Hear. Res.*, **32**, 81–92.

Gleich, O. and Wilson, S. (1993) The diameters of guinea pig auditory nerve fibres: Distribution and correlation with spontaneous rate, *Hear. Res.*, **71**, 69–79.

Goldman, L. and Albus, J. S. (1968) Computation of impulse conduction in myelinated fibres; theoretical basis of the velocity-diameter relation, *Biophys. J.*, **8**, 596–607.

Gummer, A. W. (1991) First order temporal properties of spontaneous and tone-evoked activity of auditory afferent neurones in the cochlear ganglion of the pigeon, *Hear. Res.*, **55**, 143–166.

Gummer, A. W., Smolders, J. W. T. and Klinke, R. (1987) Basilar membrane motion in the pigeon measured with the Mössbauer technique, *Hear. Res.*, **29**, 63–92.

Guofu, G. and Kaiya, Z. (1990) The number of fibers and range of fiber diameters in the cochlear nerve of three odontocete species, *Can. J. Zool.*, **69**, 2360–2364.

Karnes, J., Robb, R., O'Brien, P. C., Lamberót, E. H. and Dyck, P. J. (1977) Computerized image recognition for morphometry of nerve attribute of shape of sampled transverse sections of myelinated fibers which best estimates their average diameter, *J. Neurol. Sci.*, **34**, 43–51.

Köppl, C. (1993) Hair-cell specializations and the auditory fovea in the barn owl cochlea, In *Biophysics of Hair Cell Sensory Systems*, Duifhuis, H., Horst, J. W., van Dijk, P. and van Netten, S. M., eds., World Scientific Publishing Co., Singapore, pp. 216–222.

Köppl, C. (1994) Auditory nerve terminals in the cochlear nucleus magnocellularis: Differences between low and high frequencies, *J. Comp. Neurol.*, **339**, 438–446.

Köppl, C. (1995) Phase locking at high frequencies in the barn owl's auditory nerve, *Abstr. 18th Midw. Meetg. ARO, St. Petersburg Bch., Fla.*, 96.

Köppl, C., Gleich, O. and Manley, G. A. (1993) An auditory fovea in the barn owl cochlea, *J. Comp. Physiol. A.*, **171**, 695–704.

Landolt, J. P., Topliff, E. D. L. and Silverberg, J. D. (1972) Microscopic anatomy of the vestibular nerve in the pigeon: The size distribution of myelinated fibres, *DCIEM Report*, **858**, 1–21.

Manley, G. A. (1990) *Peripheral hearing mechanisms in reptiles and birds*, Springer Verlag, Berlin Heidelberg, 288 pages.

Manley, G. A., Gleich, O., Leppelsack, H.-J. and Oeckinghaus, H. (1985) Activity patterns of cochlear ganglion neurones in the starling, *J. Comp. Physiol. A.*, **157**, 161–181.

Manley, G. A., Brix, J. and Kaiser, A. (1987) Developmental stability of the tonotopic organization of the chick's basilar papilla, *Science*, **237**, 655–656.

Manley, G. A., Gleich, O., Kaiser, A. and Brix, J. (1989) Functional differentiation of sensory cells in the avian auditory periphery, *J. Comp. Physiol. A.*, **164**, 289–296.

Manley, G. A., Haeseler, C. and Brix, J. (1991a) Innervation patterns and spontaneous activity of afferent fibres to the lagenar macula and apical basilar papilla of the chick's cochlea, *Hear. Res.*, **56**, 211–226.

Manley, G. A., Kaiser, A., Brix, J. and Gleich, O. (1991b) Activity patterns of primary auditory-nerve fibres in chickens: Development of fundamental properties, *Hear. Res.*, **57**, 1–15.

Manley, G. A., Meyer, B., Fischer, F. P., Schwabedissen, G. and Gleich, O. (1996) Surface morphology of basilar papilla of the tufted duck *Aythya fuligula*, and domestic chicken *Gallus gallus domesticus*, *J. Morphol.*, **227**, 197–212.

Miller, M. R. (1985) Quantitative studies of auditory hair cells and nerves in lizards, *J. Comp. Neurol.*, **232**, 1–24.

Mulroy, M. J. and Oblak, T. G. (1985) Cochlear nerve of the alligator lizard, *J. Comp. Neurol.*, **233**, 463–472.

Paintal, A. S. (1966) The influence of diameter of medullated nerve fibres of cats on the rising and falling phases of the spike and its recovery, *J. Physiol.*, **184**, 791–811.

Paintal, A. S. (1967) A comparison of the nerve impulses of mammalian non-medullated nerve fibres with those of the smallest diameter medullated fibres, *J. Physiol.*, **193**, 523–533.

Parks, T. N. (1981) Morphology of axosomatic endings in an avian cochlear nucleus: Nucleus magnocellularis of the chicken, *J. Comp. Neurol.*, **203**, 425–440.

Ritchie, J. M. (1982) On the relation between fibre diameter and conduction velocity in myelinated nerve fibres, *Proc. R. Soc. Lond.*, **217**, 29–35.

Roth, B. and Bruns, V. (1993) Late developmental changes of the innervation densities of the myelinated fibres and the outer hair cell efferent fibres in the rat cochlea, *Anat. Embryol. (Berl).*, **187**, 565–571.

Rushton, W. A. H. (1951) A theory of the effects of fibre size in medullated nerve, *J. Physiol.*, **115**, 101–122.

Ryugo, D. K. (1992) The auditory nerve: Peripheral innervation, cell body morphology, and central projections, In *The Mammalian Auditory Pathway: Neuroanatomy*, Webster, D. B., Popper, A. N. and Fay, R. R., eds., Springer Verlag, New York, pp. 23–65.

Sachs, M. B., Young, E. D. and Lewis, R. H. (1974) Discharge patterns of single fibers in the pigeon auditory nerve, *Brain Res.*, **70**, 431–447.

Sachs, M. B., Woolf, N. K. and Sinnott, J. M. (1980) Response properties of neurons in the avian auditory system: Comparisons with mammalian homologues and consideration of the neural encoding of complex stimuli, In *Comparative studies of hearing in vertebrates*, Popper, A. N. and Fay, R. R., eds., Springer-Verlag, New York, Heidelberg, Berlin, pp. 323–353.

Salvi, R. J., Saunders, S. S., Powers, N. L. and Boettcher, F. A. (1992) Discharge patterns of cochlear ganglion neurons in the chicken, *J. Comp. Physiol. A.*, **170**, 227–241.

Shamma, S. A., Shen, N. and Gopalaswamy, P. (1989) Stereausis: Binaural processing without neural delays, *J. Acoust. Soc. Am.*, **86**, 989–1006.

Simmons, D. D. and Narins, P. M. (1995) Conduction velocity, fiber diameter and response latency in auditory nerve fibers of *Rana pipiens pipiens*: Toward temporal separation or coincidence? In *Nervous Systems and Behaviour*, Burrows, M., Matheson, T., Newland, P. L. and Schuppe, H., eds., Georg Thieme Verlag, Stuttgart, New York, p. 347.

Smith, C. A., Konishi, M. and Schuff, N. (1985) Structure of the Barn Owl's (*Tyto alba*) inner ear, *Hear. Res.*, **17**, 237–247.

Smith, R. S. and Koles, Z. J. (1970) Myelinated nerve fibers: computed effect of myelin thickness on conduction velocity, *Am. J. Physiol.*, **219**, 1256–1257.

Smolders, J. W. T., Ding-Pfennigdorff, D. and Klinke, R. (1995) A functional map of the pigeon basilar papilla: correlation of the properties of single auditory nerve fibres and their peripheral origin, *Hear. Res.*, **92**, 151–169.

Spoendlin, H. and Schrott, A. (1989) Analysis of the human auditory nerve, *Hear. Res.*, **43**, 25–38.

Sullivan, W. E. and Konishi, M. (1984) Segregation of stimulus phase and intensity coding in the cochlear nucleus of the barn owl, *J. Neurosci.*, **4**, 1787–1799.

Takahashi, T. and Konishi, M. (1986) Selectivity for interaural time difference in the owl's midbrain, *J. Neurosci.*, **6**, 3413–3422.

Takasaka, T. and Smith, C. A. (1971) The structure and innervation of the pigeon's basilar papilla, *J. Ultrastructure*, **35**, 20–65.

Tilney, L. G. and Tilney, M. S. (1986) Functional organization of the cytoskeleton, *Hear. Res.*, **22**, 55–77.

Vater, M., Feng, A. S. and Betz, M. (1985) An HRP-study of the frequency-place map of the horseshoe bat cochlea: Morphological correlates of the sharp tuning to a narrow frequency band, *J. Comp. Physiol. A*, **157**, 671–686.

Waxman, S. G. and Bennett, M. V. L. (1972) Relative conduction velocities of small myelinated and non-myelinated fibres in the central nervous system, *Nature*, **238**, 217–219.

Whitehead, M. C. and Morest, D. K. (1981) Dual populations of efferent and afferent cochlear axons in the chicken, *Neuroscience*, **6**, 2351–2365.

Winter, P. (1963) Vergleichende qualitative und quantitative Untersuchungen an der Hörbahn von Vögeln. *Z. Morphol, Ökol. Tiere*, **52**, 365–400.

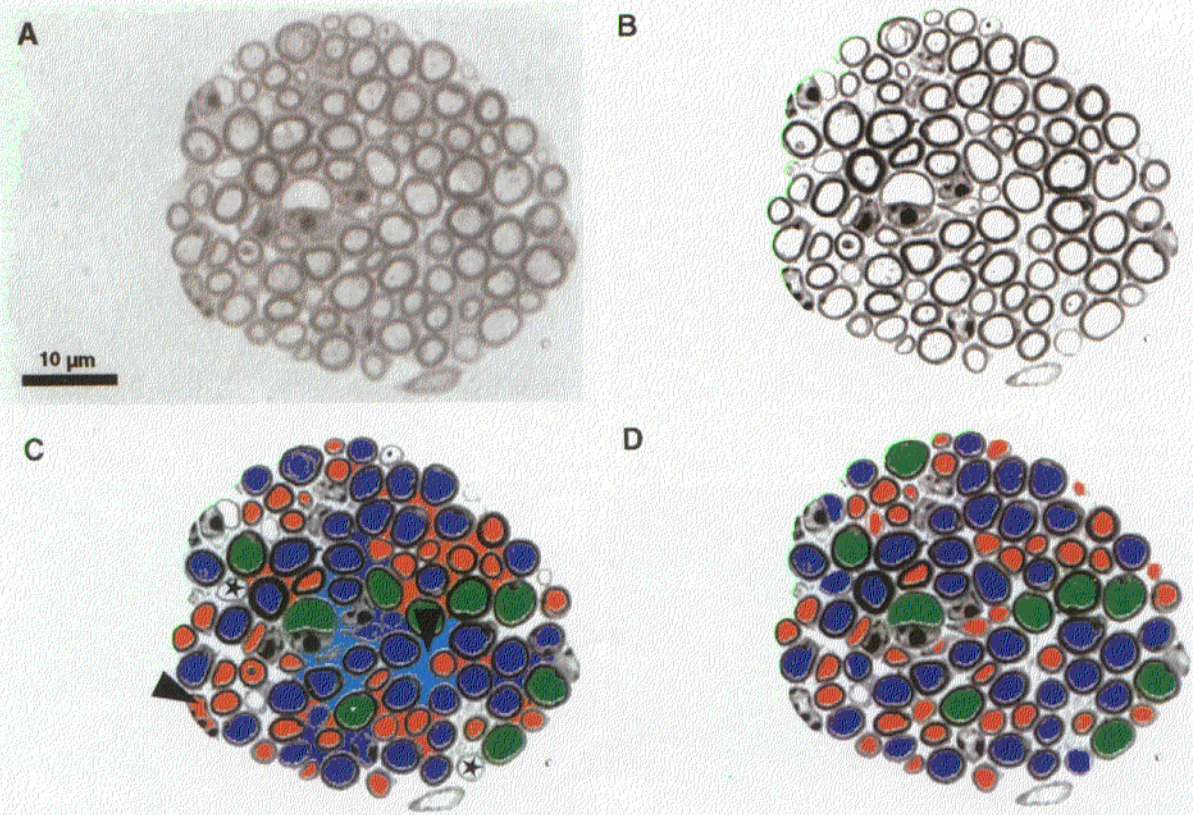

Colour Plate I (See page 316, Figure 1) Example of the major steps of the semi-automated image analysis used to define axons in peripheral semi-thin sections that only contained lagenar fibres. Each image shows about half the area visible on the video monitor, using a ×100 objective on the microscope. **A**: Digitized microscope image. **B**: The same image as in A, but after digital sharpening and contrast enhancement. **C**: The same image as B, with a colour overlay, showing individual particles covering areas of a custom-defined range of grey values. The different colouring according to diameter is simply a visual aid and bears no importance for further analysis. Note some errors, i.e., particles that are not axons (two examples marked with arrowheads) and axons not detected (two examples marked with asterisks). **D**: The same image as in C, but after interactive correction of detection errors. At this stage, particle parameters were measured automatically and stored.

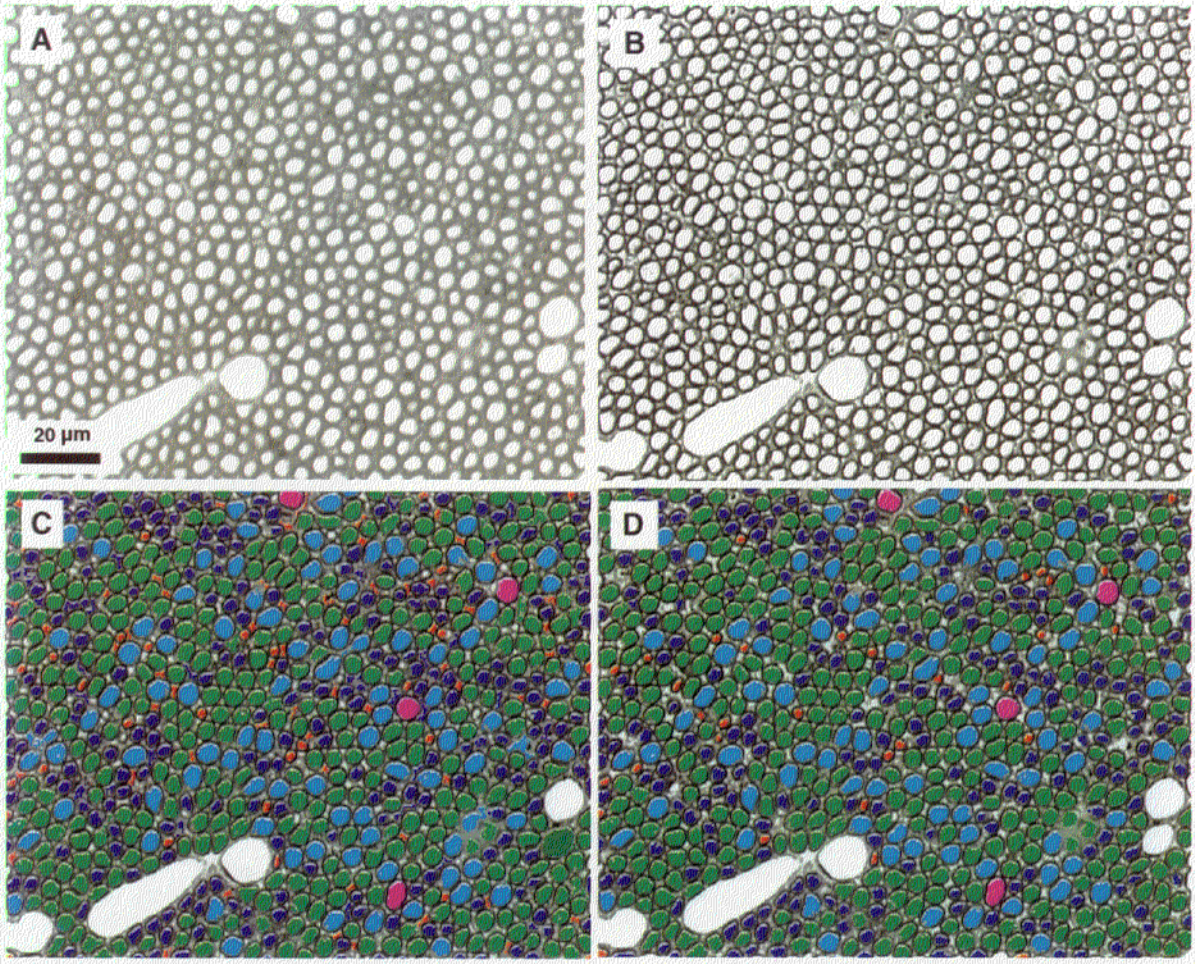

Colour Plate II (See page 317, Figure 2) Example of major steps of the semi-automated image analysis used to define axons in most semi-thin sections. Each image shows about half the area visible on the video monitor, using a x40 objective on the microscope. Panel layout is the same as in Figure 1. The large objects that were left undetected are blood vessels.

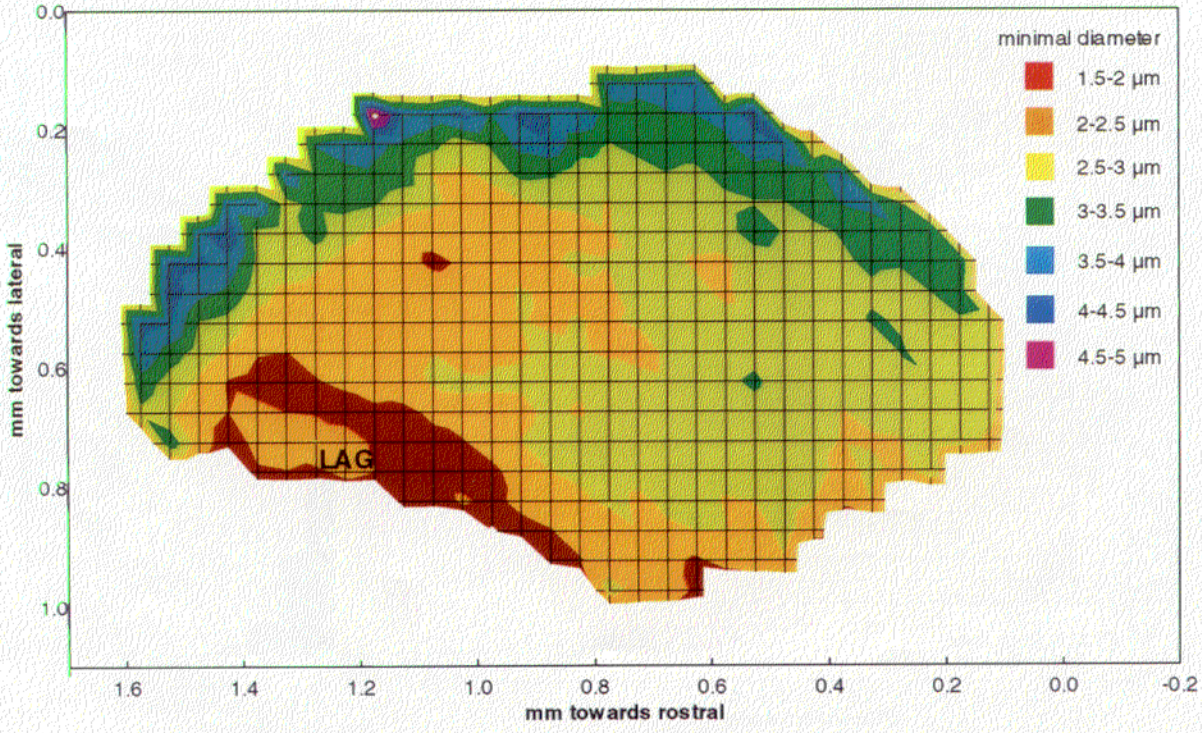

Colour Plate III (See page 325, Figure 9) Example of the distribution of axon minimal diameters in central sections, shown as a colour-coded contour plot. The outline of the section is reproduced to scale, with the anatomical axes indicated by the ordinate and abscissa. Areas within the section are coloured according to the minimal diameter average over small squares of 50 × 50 µm; these squares are indicated by a fine grid, the colour code is explained in the legend (note that the red-brown areas representing diameters of 1.5-2 µm do not exactly match the brighter red in the legend). The area marked "LAG" indicates the approximate position of the lagenar fibre group. This thin halo of apparently small diameters adjacent to the large ones along the medial edge of the nerve is an artefact of the plotting procedure.

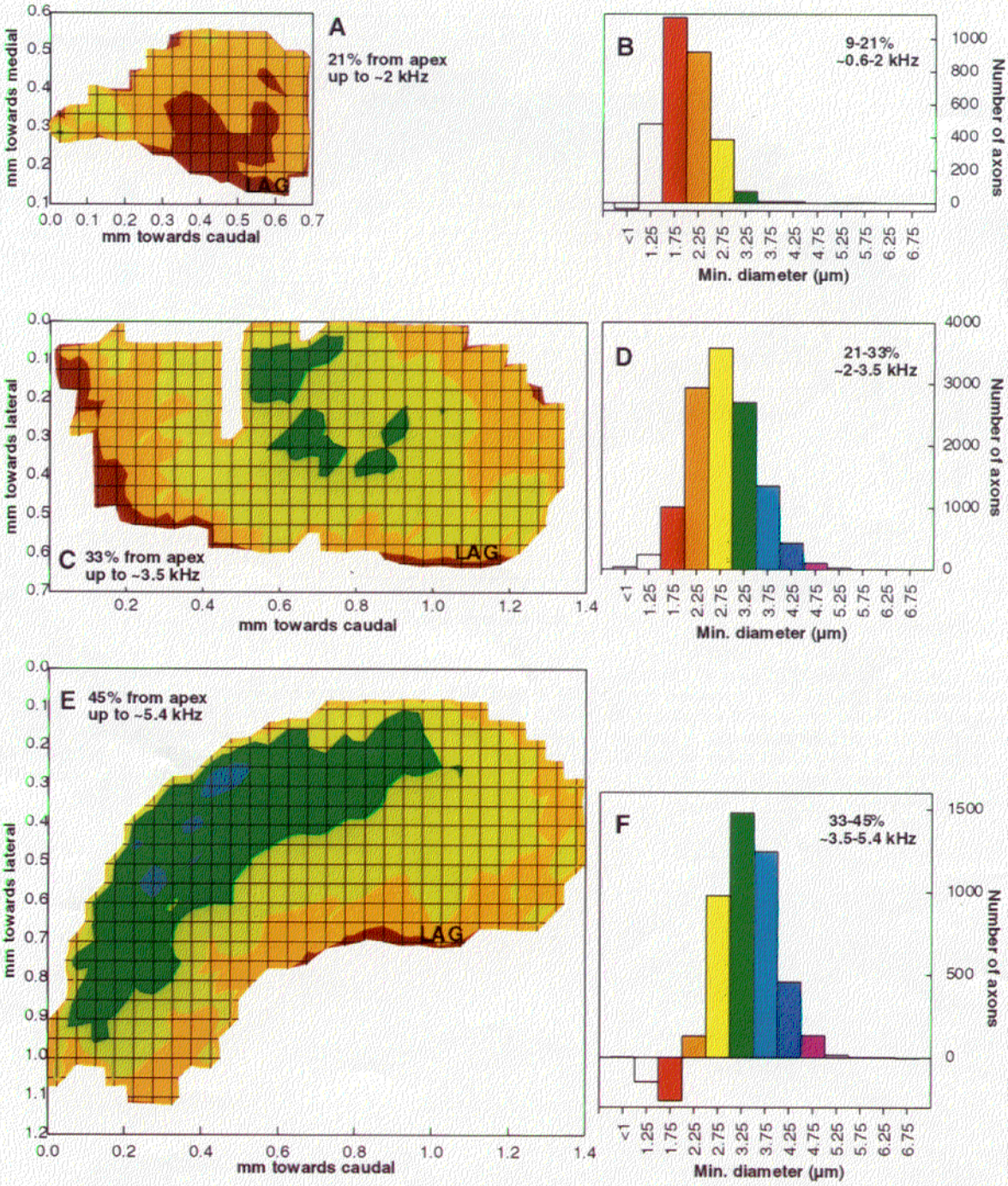

Colour Plate IV (See page 326, Figure 10) Distributions of axon minimal diameters in a series of sections from the apex to the base of the basilar papilla and the nerve as indicated in Figure 3. Panels A ,C ,E ,G and J are the contour plots with the same layout and the same colour code as Figure 9. All contour plots are drawn to the same scale and are oriented alike. Panels B, D, F, H, I and K show the differences in the distributions of minimal diameters between successive sections whose position and approximate frequency range are indicated. Their bin classification and colour code also correspond to the legend in Figure 9 (note that the bright red of the bars representing diameters of 1.5-2 µm does not exactly match the more brownish red of the corresponding areas in the contour plots); bins shown in white are not represented in the contour plots if the corresponding axons were at the edge of the nerve.

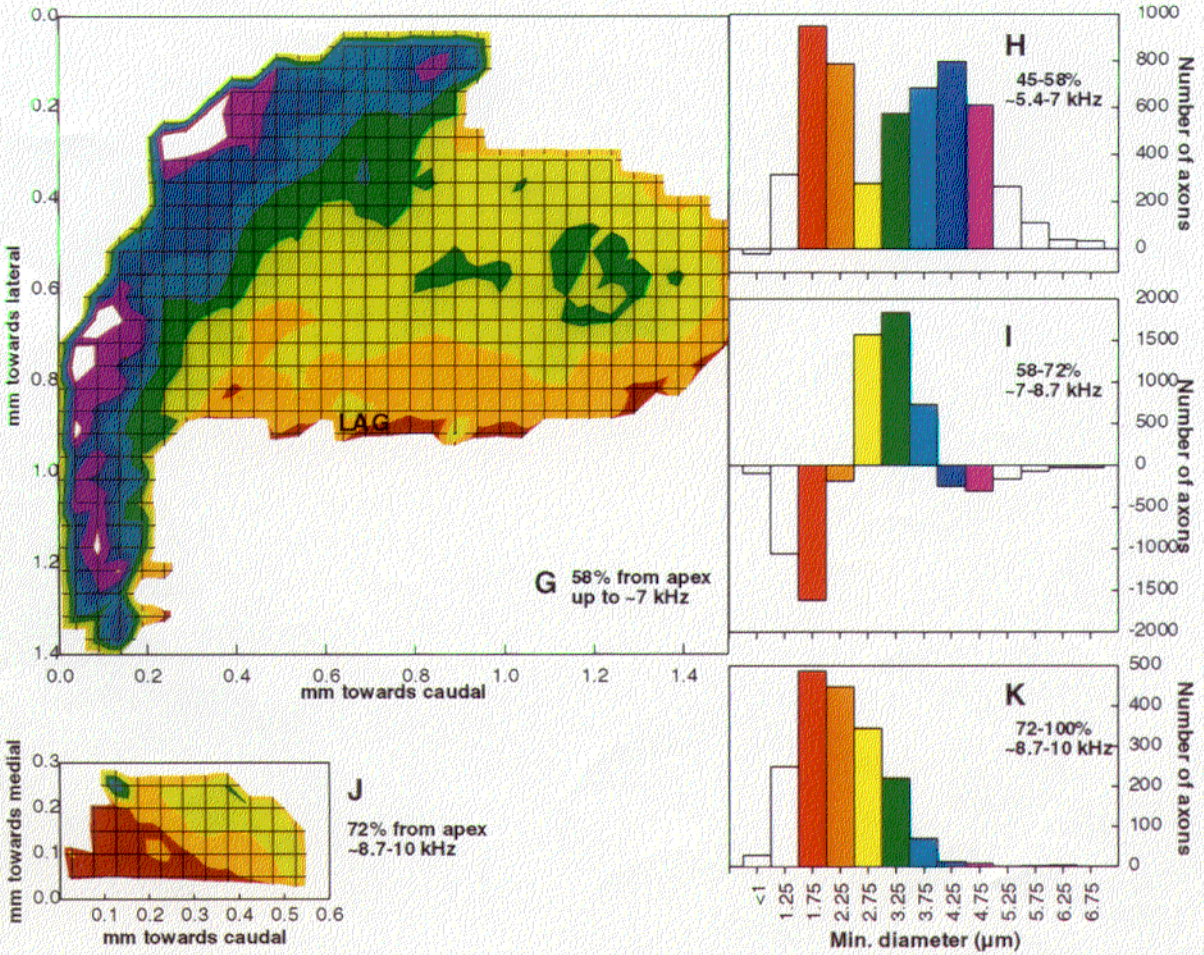

Colour Plate V (See page 327, Figure 10 continued)